PCR as described previously [17]. Primers used in this study are summarized in Additional file 1. The first round of PCR was performed on each cDNA template using 10 nM of each of the following primers: a target protein specific primer (5'-CCACCCACCACCACCAatgnnnnnnnnn nnnnnnnn-3'; lowercase indicates the 5'-coding region of the target gene) and the AODA2306 primer. Then, a second round of PCR was carried out to construct the templates for protein synthesis using a portion (5 μl) of the first PCR mix, 100 nM SPu primer, 100 nM AODA2303 primer and 1 nM deSP6E02 primer. GST tags were used according to the methods we described previously [17]. The transcription templates of two HECT-type E3 ligases, UPL7 and UPL5, were generated as C-terminal FLAG-tagged proteins using the Gateway System® (Invitrogen, Carlsbad, CA, USA). Briefly, the ORF sequences of UPL7 and UPL5 were amplified by PCR with sense and antisense primers containing attB1 and FLAG-attB2 sequences, respectively. According to the manufacturer's instructions (Invitrogen), these DNA fragments were subcloned into pDONR221 vector by BP reaction and then inserted into the Gateway-based pEU vector (pEU-E01-GW) by LR reaction. Using these recombinant vectors as templates, PCR was carried out with 100 nM SPu primer and 100 nM AODA2303 primer and used as transcription templates.

Cell-free Protein Synthesis

In vitro transcription and cell-free protein synthesis were performed as described [18]. Transcript was made from each of the DNA templates mentioned above using the SP6 RNA polymerase. The synthetic mRNAs were then precipitated with ethanol and collected by centrifugation using a Hitachi R10H rotor. Each mRNA (usually 30–35 μg) was washed and transferred into a translation mixture. The translation reaction was performed in the bilayer mode [35] with slight modifications. The translation mixture that formed the bottom layer consisted of 60 A260 units of the wheat germ extract (CellFree Sciences, Yokohama, Japan) and 2 μg creatine kinase (Roche Diagnostics K. K., Tokyo, Japan) in 25 μl of SUB-AMIX® (CellFree Sciences). The SUB-AMIX® contained (final concentrations) 30 mM Hepes/KOH at pH 8.0, 1.2 mM ATP, 0.25 mM GTP, 16 mM creatine phosphate, 4 mM DTT, 0.4 mM spermidine, 0.3 mM each of the 20 amino acids, 2.7 mM magnesium acetate, and 100 mM potassium acetate. SUB-AMIX® (125 μl) was placed on the top of the translation mixture, forming the upper layer. After incubation at 16°C for 15 h, the synthesized proteins were confirmed by SDS-PAGE. For biotin labeling, 1 μl of crude biotin ligase (BirA) produced by the wheat cell-free expression system was added to the bottom layer, and 0.5 μM (final concentration) of D-biotin (Nacalai Tesque, Inc., Kyoto, Japan) was added to both upper and bottom layers, as described previously [22].

Purification of E2 and E3 Proteins

Purification of GST-tagged protein was carried out according to the procedure described previously [36] with slight modification. Crude GST-tagged recombinant protein (450 μl) produced by the cell-free reaction was precipitated with glutathione sepharose™ 4B (GE Healthcare, Buckinghamshire, UK). The recombinant proteins were eluted with PBS buffer containing 0.1 U of AcTEV protease (Invitrogen) in order to cleave the GST tag from the protein.

Detection of Polyubiquitination by the Luminescent Method

In vitro polyubiquitination assays were carried out in a total volume of 15 μl consisting of 20 mM Tris-HCl pH 7.5, 0.2 mM DTT, 5 mM $MgCl_2$, (10 μM zinc acetate in the assays for RING-type E3s only), 3 mM ATP, 1 mg/ml BSA, 25 nM biotinylated ubiquitin, 25 nM FLAG-tagged ubiquitin, 1 μl of recombinant E2 (purified or crude) and 1 μl of recombinant E3 (purified or crude) in the presence or absence of 0.05 μM rabbit E1 (Boston Biochem, Cambridge, MA, USA) at 30°C for 1 hr in a 384-well Optiplate (PerkinElmer, Boston, MA, USA). In accordance with the AlphaScreen IgG (ProteinA) detection kit (Perkin Elmer) instruction manual, 10 μl of detection mixture containing 20 mM Tris-HCl pH 7.5, 0.2 mM DTT, 5 mM $MgCl_2$, 5 μg/ml Anti-FLAG antibody (Sigma-Aldrich, St. Louis, MO, USA), 1 mg/ml BSA, 0.1 μl streptavidin-coated donor beads and 0.1 μl anti-IgG acceptor beads were added to each well of the 384 Optiplate followed by incubation at 23°C for 1 hr. Luminescence was analyzed by the AlphaScreen detection program.

Detection of Ubiquitinated E2 by Immunoblot Analysis

Crude biotinylated recombinant E2 proteins (40 μl) were used for the ubiquitin-conjugating assay in a total reaction volume of 50 μl containing 20 mM Tris-HCl pH 7.5, 0.2 mM DTT, 5 mM $MgCl_2$, 3 mM ATP and 4 μM FLAG-tagged ubiquitin (Sigma) for 3 hr at 30°C. The reaction products were purified by Streptavidin Magnesphere Paramagnetics particles (Promega, Madison, WI, USA). After washing the beads with PBS buffer, recombinant E2s were boiled in 15 μl of SDS sample buffer containing 50 mM Tris-HCl pH 6.8, 2% SDS, 10% glycerol and 0.2% bromophenol blue, and then separated from the magnet beads. The proteins were separated by SDS-PAGE and transferred to PVDF membrane (Millipore Bedford, MA, USA) according to standard procedures. The blots were detected by the ECL plus detection system (GE Healthcare) with anti-FLAG antibody (Sigma) according to the manufacturer's procedure.

Detection of Polyubiquitination by the Immunoblot Analysis

For polyubiquitination of HECT-type E3 ligases, crude FLAG-tagged UPL recombinant protein (20 μl) was ubiq-

uitinated in a total reaction volume of 50 μl consisting of 20 mM Tris-HCl pH 7.5, 0.2 mM DTT, 5 mM $MgCl_2$, 3 mM ATP, 4 μM biotinylated ubiquitin and 20 μl of crude recombinant AtUBC8 for 3 hr at 30°C. Then, recombinant UPL protein was gathered by anti-FLAG M2 agarose (Sigma). After washing the agarose with PBS buffer, the recombinant UPL protein was boiled in 15 μl of SDS sample buffer and then separated from beads by centrifugation. For polyubiquitination of RING-type E3 ligases, the assay was carried out in 10 μl of reaction mixture containing 20 mM Tris-HCl pH 7.5, 0.2 mM DTT, 5 mM $MgCl_2$, 10 μM zinc acetate, 3 mM ATP, 1 mg/ml BSA, 4 μM FLAG- or His-tagged ubiquitin, 1 μl of purified or crude recombinant E2 and 1 μl of purified or crude recombinant E3 at 30°C for 3 hr. Then, 5 μl of three-fold concentrated SDS sample buffer was added to the reaction mixture and boiled for 5 min. Proteins were separated by SDS-PAGE and transferred to Hybond-LFP PVDF membrane (GE Healthcare) according to standard procedures. Immunoblot analysis was carried out with anti-FLAG antibody (Sigma) or anti-His antibody (GE Healthcare) according to the procedure described above. When detecting biotinylated ubiquitin, blots were treated with 5 μg/ml Alexa488-conjugated streptavidin (Invitrogen) in PBS buffer. After washing with PBS containing 0.1% Tween-20, the blot was analyzed by a Typhoon Imager (GE Healthcare) using the 532 nm laser and 526 emission filters.

Polyubiquitination Assay with 26S Proteasome Inhibitor

Polyubiquitination reaction was carried out as same procedure described above except addition of MG132 (Calbiochem, San Diego, CA, USA) at a final concentration of 20 μM to reaction mixture. Then, the protein on blot was detected by immunoblot analysis with anti-FLAG antibody or Alexa488-conjugated streptavidin.

Authors' contributions

HT conceived the study and performed the experiments, and contributed to writing the manuscript. MS and KS provided RAFL cDNA clones. AN conceived the study. YE conceived the study and supervised the work. TS conceived and designed the study, supervised the work and contributed to writing the manuscript.

Additional material

Additional file 1

AGI code of Arabidopsis genes and primer sequences used in this study.

AGI code of Arabidopsis genes and primer sequences used in this study. Click here for file [http://www.biomedcentral.com/content/supplementary/1471-2229-9-39-S1.xls]

Acknowledgements

This work was partially supported by the Special Coordination Funds for Promoting Science and Technology by the Ministry of Education, Culture, Sports, Science and Technology, Japan (T. S. and Y. E.). We thank Michael Andy Goren for proofreading this manuscript.

References

1. Bai C, Sen P, Hofmann K, Ma L, Goebl M, Harper JW, Elledge SJ: **SKP1 Connects Cell Cycle Regulators to the Ubiquitin Proteolysis Machinery through a Novel Motif, the F-Box.** *Cell* 1996, **86(2):**263-274.
2. Chen Z, Hagler J, Palombella VJ, Melandri F, Scherer D, Ballard D, Maniatis T: **Signal-induced site-specific phosphorylation targets IκBα to the ubiquitin-proteasome pathway.** *Genes Dev* 1995, **9(13):**1586-1597.
3. Pickart CM: **Mechanisms underlying ubiquitination.** *Annu Rev Biochem* 2001, **70:**503-533.
4. Smalle J, Vierstra RD: **The ubiquitin 26S proteasome proteolytic pathway.** *Annu Rev Plant Biol* 2004, **55:**555-590.
5. Borden KL: **RING domains: master builders of molecular scaffolds?** *J Mol Biol* 2000, **295(5):**1103-1112.
6. Glickman MH, Ciechanover A: **The ubiquitin-proteasome proteolytic pathway: destruction for the sake of construction.** *Physiol Rev* 2002, **82(2):**373-428.
7. Schnell JD, Hicke L: **Non-traditional functions of ubiquitin and ubiquitin-binding proteins.** *J Biol Chem* 2003, **278(38):**35857-35860.
8. Hofmann RM, Pickart CM: **Noncanonical MMS2-encoded ubiquitin-conjugating enzyme functions in assembly of novel polyubiquitin chains for DNA repair.** *Cell* 1999, **96(5):**645-653.
9. Yin XJ, Volk S, Ljung K, Mehlmer N, Dolezal K, Ditengou F, Hanano S, Davis SJ, Schmelzer E, Sandberg G, Teige M, Palme K, Pickart C, Bachmair A: **Ubiquitin lysine 63 chain forming ligases regulate apical dominance in Arabidopsis.** *Plant Cell* 2007, **19(6):**1898-1911.
10. Hicke L: **A new ticket for entry into budding vesicles – ubiquitin.** *Cell* 2001, **106(5):**527-530.
11. Vierstra RD: **The ubiquitin/26S proteasome pathway, the complex last chapter in the life of many plant proteins.** *Trends Plant Sci* 2003, **8(3):**135-142.
12. Nelson DC, Lasswell J, Rogg LE, Cohen MA, Bartel B: **FKF1, a Clock-Controlled Gene that Regulates the Transition to Flowering in Arabidopsis.** *Cell* 2000, **101(3):**331-340.
13. Osterlund MT, Hardtke CS, Wei N, Deng XW: **Targeted destabilization of HY5 during light-regulated development of Arabidopsis.** *Nature* 2000, **405(6785):**462-466.
14. Stone SL, Williams LA, Farmer LM, Vierstra RD, Callis J: **KEEP ON GOING, a RING E3 ligase essential for Arabidopsis growth and development, is involved in abscisic acid signaling.** *Plant Cell* 2006, **18(12):**3415-3428.
15. Rosebrock TR, Zeng L, Brady JJ, Abramovitch RB, Xiao F, Martin GB: **A bacterial E3 ubiquitin ligase targets a host protein kinase to disrupt plant immunity.** *Nature* 2007, **448(7151):**370-374.
16. Kraft E, Stone SL, Ma L, Su N, Gao Y, Lau OS, Deng XW, Callis J: **Genome analysis and functional characterization of the E2 and RING-type E3 ligase ubiquitination enzymes of Arabidopsis.** *Plant Physiol* 2005, **139(4):**1597-1611.
17. Sawasaki T, Ogasawara T, Morishita R, Endo Y: **A cell-free protein synthesis system for high-throughput proteomics.** *Proc Natl Acad Sci USA* 2002, **99(23):**14652-14657.
18. Sawasaki T, Gouda MD, Kawasaki T, Tsuboi T, Tozawa Y, Takai K, Endo Y: **The wheat germ cell-free expression system: methods for high-throughput materialization of genetic information.** *Methods Mol Biol* 2005, **310:**131-144.
19. Kobayashi T, Kodani Y, Nozawa A, Endo Y, Sawasaki T: **DNA-binding profiling of human hormone nuclear receptors via fluorescence correlation spectroscopy in a cell-free system.** *FEBS Lett* 2008, **582(18):**2737-2744.
20. Seki M, Narusaka M, Kamiya A, Ishida J, Satou M, Sakurai T, Nakajima M, Enju A, Akiyama K, Oono Y, Muramatsu M, Hayashizaki Y, Kawai J, Carninci P, Itoh M, Ishii Y, Arakawa T, Shibata K, Shinagawa A, Shinozaki K: **Functional annotation of a full-length Arabidopsis cDNA collection.** *Science* 2002, **296(5565):**141-145.
21. Kus B, Gajadhar A, Stanger K, Cho R, Sun W, Rouleau N, Lee T, Chan D, Wolting C, Edwards A, Bosse R, Rotin D: **A high throughput**

screen to identify substrates for the ubiquitin ligase Rsp5. *J Biol Chem* 2005, **280(33):**29470-29478.
22. Sawasaki T, Kamura N, Matsunaga S, Saeki M, Tsuchimochi M, Morishita R, Endo Y: **Arabidopsis HY5 protein functions as a DNA-binding tag for purification and functional immobilization of proteins on agarose/DNA microplate.** *FEBS Lett* 2008, **582(2):**221-228.
23. Bates PW, Vierstra RD: **UPL1 and 2, two 405 kDa ubiquitin-protein ligases from Arabidopsis thaliana related to the HECT-domain protein family.** *Plant J* 1999, **20(2):**183-195.
24. Downes BP, Stupar RM, Gingerich DJ, Vierstra RD: **The HECT ubiquitin-protein ligase (UPL) family in Arabidopsis: UPL3 has a specific role in trichome development.** *Plant J* 2003, **35(6):**729-742.
25. Stone SL, Hauksdóttir H, Troy A, Herschleb J, Kraft E, Callis J: **Functional analysis of the RING-type ubiquitin ligase family of Arabidopsis.** *Plant Physiol* 2005, **137(1):**13-30.
26. Hardtke CS, Okamoto H, Deng XW: **Biochemical evidence for ubiquitin ligase activity of the Arabidopsis COP1 interacting protein 8 (CIP8).** *Plant J* 2002, **30(4):**385-394.
27. Yamauchi K, Wada K, Tanji K, Tanaka M, Kamitani T: **Ubiquitination of E3 ubiquitin ligase TRIMa and its potential role.** *FEBS J* 2008, **275(7):**1540-1555.
28. Waxman L, Fagan JM, Goldberg AL: **Demonstration of two distinct high molecular weight proteases in rabbit reticulocytes, one of which degrades ubiquitin conjugates.** *J Biol Chem* 1987, **262(6):**2451-2457.
29. Chen ZJ, Parent L, Maniatis T: **Site-Specific Phosphorylation of IκBα by a Novel Ubiquitination-Dependent Protein Kinase Activity.** *Cell* 1996, **84(6):**853-862.
30. Hatfield PM, Vierstra RD: **Ubiquitin-dependent proteolytic pathway in wheatgerm: Isolation of multiple forms of ubiquitin-activating enzyme, E1.** *Biochemistry* 1989, **28:**735-742.
31. Wu CJ, Conze DB, Li T, Srinivasula SM, Ashwell JD: **Sensing of Lys 63-linked polyubiquitination by NEMO is a key event in NF-κB activation.** *Nature Cell Biol* 2006, **8(4):**398-406.
32. Yin XJ, Volk S, Ljung K, Mehlmer N, Dolezal K, Ditengou F, Hanano S, Davis SJ, Schmelzer E, Sandberg G, Teige M, Palme K, Pickart C, Bachmaira A: **Ubiquitin lysine 63 chain-forming ligases regulate apical dominance in Arabidopsis.** *Plant Cell* 2007, **19(6):**1898-1911.
33. Madin K, Sawasaki T, Ogasawara T, Endo Y: **A highly efficient and robust cell-free protein synthesis system prepared from wheat embryos: Plants apparently contain a suicide system directed at ribosomes.** *Proc Natl Acad Sci USA* 2000, **97(2):**559-564.
34. Li W, Tu D, Brunger AT, Ye Y: **A ubiquitin ligase transfers preformed polyubiquitin chains from a conjugating enzyme to a substrate.** *Nature* 2007, **446(7133):**333-337.
35. Sawasaki T, Hasegawa Y, Tsuchimochi M, Kamura N, Ogasawara T, Kuroita T, Endo Y: **A bilayer cell-free protein synthesis system for high-throughput screening of gene products.** *FEBS Lett* 2002, **514(1):**102-105.
36. Masaoka T, Nishi M, Ryo A, Endo Y, Sawasaki T: **The wheat germ cell-free based screening of protein substrates of calcium/calmodulin-dependent protein kinase II delta.** *FEBS Lett* 2008, **582(13):**1795-1801.

OPEN ACCESS Freely available online

PLoS one

Hepatitis C Virus Core Protein Abrogates the DDX3 Function That Enhances IPS-1-Mediated IFN-Beta Induction

Hiroyuki Oshiumi[1], Masanori Ikeda[2], Misako Matsumoto[1], Ayako Watanabe[1], Osamu Takeuchi[3], Shizuo Akira[3], Nobuyuki Kato[2], Kunitada Shimotohno[4], Tsukasa Seya[1]*

1 Department of Microbiology and Immunology, Hokkaido University Graduate School of Medicine, Sapporo, Japan, **2** Department of Tumor Virology, Okayama University Graduate School of Medicine, Dentistry, and Pharmaceutical Sciences, Okayama, Japan, **3** Laboratory of Host Defense, WPI Immunology Frontier Research Center, Research Institute for Microbial Diseases, Osaka University, Suita, Japan, **4** Research Institute, Chiba Institute of Technology, Narashino, Japan

Abstract

The DEAD box helicase DDX3 assembles IPS-1 (also called Cardif, MAVS, or VISA) in non-infected human cells where minimal amounts of the RIG-I-like receptor (RLR) protein are expressed. DDX3 C-terminal regions directly bind the IPS-1 CARD-like domain as well as the N-terminal hepatitis C virus (HCV) core protein. DDX3 physically binds viral RNA to form IPS-1-containing spots, that are visible by confocal microscopy. HCV polyU/UC induced IPS-1-mediated interferon (IFN)-beta promoter activation, which was augmented by co-transfected DDX3. DDX3 spots localized near the lipid droplets (LDs) where HCV particles were generated. Here, we report that HCV core protein interferes with DDX3-enhanced IPS-1 signaling in HEK293 cells and in hepatocyte Oc cells. Unlike the DEAD box helicases RIG-I and MDA5, DDX3 was constitutively expressed and colocalized with IPS-1 around mitochondria. In hepatocytes (O cells) with the HCV replicon, however, DDX3/IPS-1-enhanced IFN-beta-induction was largely abrogated even when DDX3 was co-expressed. DDX3 spots barely merged with IPS-1, and partly assembled in the HCV core protein located near the LD in O cells, though in some O cells IPS-1 was diminished or disseminated apart from mitochondria. Expression of DDX3 in replicon-negative or core-less replicon-positive cells failed to cause complex formation or LD association. HCV core protein and DDX3 partially colocalized only in replicon-expressing cells. Since the HCV core protein has been reported to promote HCV replication through binding to DDX3, the core protein appears to switch DDX3 from an IFN-inducing mode to an HCV-replication mode. The results enable us to conclude that HCV infection is promoted by modulating the dual function of DDX3.

Citation: Oshiumi H, Ikeda M, Matsumoto M, Watanabe A, Takeuchi O, et al. (2010) Hepatitis C Virus Core Protein Abrogates the DDX3 Function That Enhances IPS-1-Mediated IFN-Beta Induction. PLoS ONE 5(12): e14258. doi:10.1371/journal.pone.0014258

Editor: Jörn Coers, Duke University Medical Center, United States of America

Received May 28, 2010; **Accepted** November 16, 2010; **Published** December 8, 2010

Funding: This work was supported in part by the Program of Founding Research Centers for Emerging and Reemerging Infectious Diseases, MEXT, Sapporo Biocluster "Bio-S", the Knowledge Cluster Initiative of the MEXT, Grants-in-Aid from the Ministry of Education, Science, and Culture (Specified Project for Advanced Research) and the Ministry of Health, Labor, and Welfare of Japan, Mochida Foundation, Yakult Foundation, NorthTec Foundation and Waxman Foundation. The funders had no role in study design, data collection and analysis, decision to publish, or preparation of the manuscript.

Competing Interests: The authors have declared that no competing interests exist.

* E-mail: seya-tu@pop.med.hokudai.ac.jp

Introduction

The retinoic acid inducible gene-I (RIG-I) and the melanoma differentiation-associated gene 5 (MDA5) encode cytoplasmic RNA helicases [1–3] that signal the presence of viral RNA through the adaptor, IPS-1/Mitochondrial antiviral signaling protein (MAVS)/Caspase recruitment domain (CARD) adaptor inducing interferon (IFN)-beta (Cardif)/Virus-induced signaling adaptor (VISA) to produce IFN-beta [4–7]. IPS-1 is localized to the mitochondrial outer membrane through its C-terminus [6]. Increasing evidence suggests that the DEAD-box RNA helicase DDX3, which is on the X chromosome, participates in the regulation of type I IFN induction by the RIG-I pathway.

DDX3 acts on the IFN-inducing pathway by a complex mechanism. Early studies reported that DDX3 up-regulates IFN-beta induction by interacting with IKKepsilon [8] or TBK1 [9] in a kinase complex. Both TBK1 and IKKepsilon are IRF-3-activating kinases with NF-kappaB- and IFN-inducible properties. DDX3 has been proposed to bind IKKepsilon, and IKKepsilon is generated after NF-kappaB activation [10]. Yeast two-hybrid studies demonstrated that DDX3 binds IPS-1, and both are constitutively present prior to infection (Fig. 1). Ultimately, DDX3 forms a complex with the DEAD-box RNA helicases RIG-I and MDA5 [11], which are present at only low amounts in resting cells, and are up-regulated during virus infection. Previously we used gene silencing and disruption, to show that the main function of DDX3 is to interact with viral RNA and enhance RIG-I signaling upstream of NAP1/TBK1/IKKepsilon [11]. Hence, DDX3 is involved in multiple pathways of RNA sensing and signaling during viral infection.

DDX3 resides in both the nucleus and the cytoplasm [12], and has been implicated in a variety of processes in gene expression regulation, including transcription, splicing, mRNA export, and translation [13]. A recent report suggested that the N-terminus of hepatitis C virus (HCV) core protein binds the C-terminus of DDX3 (Fig. S1) [14,15], and this interaction is required for HCV replication [16]. Although DDX3 promotes efficient HCV infection by accelerating HCV RNA replication, the processes

A

Two representative polyI:C-binding proteins identified by mass-spectrometric analysis

dsRNA-binding protein	ID	Mr (kDa)	polyI:C	polyU	gene name
dsRNA-activated protein kinase	IPI00019463	63 kDa	37	2	PKR
ATP-dependent RNA helicase	IPI00215637	73 kDa	19	12	DDX3

B

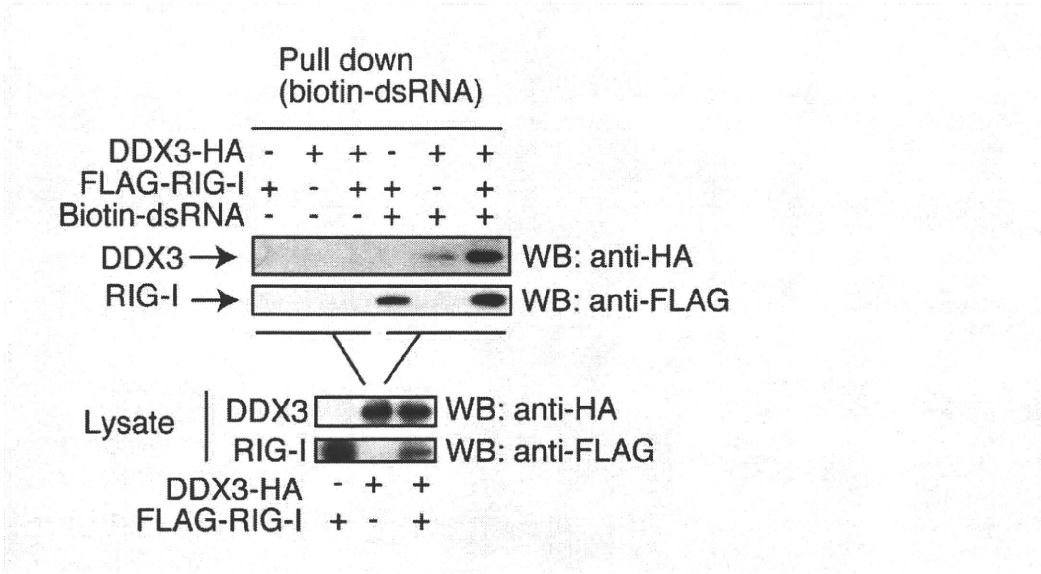

Figure 1. DDX3 is a RNA-binding protein. (A) DDX3 is a polyU- and polyI:C-binding protein. Mass spectrometry analyses indicated that DDX3 binds polyI:C- and polyU-Sepharose, although PKR binds polyI:C but not polyU. The rough data from MASCOT and one representative of six trials are shown. (B) DDX3 binds dsRNA, RIG-I and HCV core protein. Expression vectors for Flag-tagged RIG-I and HA-tagged DDX3 were transfected into HEK293 cells using lipofectamine 2000. Twenty-four hours after the transfection, extract from transfected cells were mixed with biotin-conjugated dsRNA. RNA-protein complex were recovered by pull-down assay using streptavidin-Sepharose. The protein within the pull-down fraction was analyzed by western blotting. The results are representative of two independent experiments.
doi:10.1371/journal.pone.0014258.g001

appear independent of its interaction with the viral core protein [15]. HCV seems to co-opt DDX3, and require DDX3 for replication. In addition, the association between DDX3 and core protein implicates DDX3 in HCV-related hepatocellular carcinoma progression [17]. Therefore, DDX3 could be a novel target for the development of drugs against HCV [18].

A number of reports have demonstrated the formation of the DDX3-core protein complex in the cytoplasm, but the functional relevance of DDX3-core protein interaction is not known. In this report, we show evidence that the HCV core protein participates in suppression of DDX3-augmented IPS-1 signaling for IFN-β induction. Several possible functions of DDX3 are discussed, focusing on its core protein association and IPS-1-regulatory properties.

Materials and Methods

Cell culture and reagents

HEK293 cells and HEK293FT cells were maintained in Dulbecco's Modified Eagle's low or high glucose medium (Invitrogen, Carlsbad, CA) supplemented with 10% heat-inactivated FCS (Invitrogen) and antibiotics. Huh7.5 cells were maintained in MEM (Nissui, Tokyo, Japan) supplemented with 10% heat-inactivated FCS. Hepatocyte sublines with HCV replicon (O cells) and without replicon (Oc cells) were established as described previously [19]. O cells with core-less subgenomic replicon (sO cells) were also generated in Dr. Kato's laboratory [16,19]. RIG-I −/− mouse embryonic fibroblasts (MEF) were gifts from Drs. Takeuchi and Akira [1]. Anti-FLAG M2 monoclonal Ab and anti-HA polyclonal Ab were purchased from Sigma. A mitochondria marker (Mitotracker) and Alexa Fluor®-conjugated secondary antibodies were purchased from Molecular probe. Anti-HCV core mAb (C7-50) [20] and anti-human DDX3 pAb were from Affinity BioReagents, Inc and Abcam, Cambridge MA, respectively.

Plasmids

DDX3 cDNA encoding the entire ORF was cloned into pCR-blunt vector using primers, DDX3N F-Xh (CTC GAG CCA CCA TGA GTC ATG TGG CAG TGG AA) and DDX3C R-Ba (GGA TCC GTT ACC CCA CCA GTC AAC CCC) from human lung cDNA library. To make an expression plasmid, HA tag was fused at the C-terminal end of the full length DDX3 (pEF-BOS DDX3-HA). pEF-BOS DDX3 (1-224aa) vector was made by using primers,

DDX3 N-F-Xh and DDX3D1 (GGA TCC GGC ACA AGC CAT CAA GTC TCT TTT C). pEF-BOS DDX3-HA (225-662) was made by using primers, DDX3D2-3 (CTC GAG CCA CCA TGC AAA CAG GGT CTG GAA AAA C) and DDX3C R-Ba. To make pEF-BOS DDX3-HA (225-484) and pEF-BOS DDX3-HA (485-663), the primers, DDX3D2 R-Ba (GGA TCC AAG GGC CTC TTC TCT ATC CCT C) and DDX3D3 F-Xh (CTC GAG CCA CCA TGC ACC AGT TCC GCT CAG GAA AAA G) were used, respectively. HCV core expressing plasmids, pcDNA3.1 HCVO core or JFH1 core, were previously reported by N. Kato (Okayama University Japan) [16]. Another 1b genotype of the core was cloned from a HCV patient in Osaka Medical Center (Osaka) according to the recommendation of the Ethical Committee in Osaka. We obtained written informed consent from each patient for research use of their samples. Reporter and internal control plasmids for reporter gene assay are previously described [21,22].

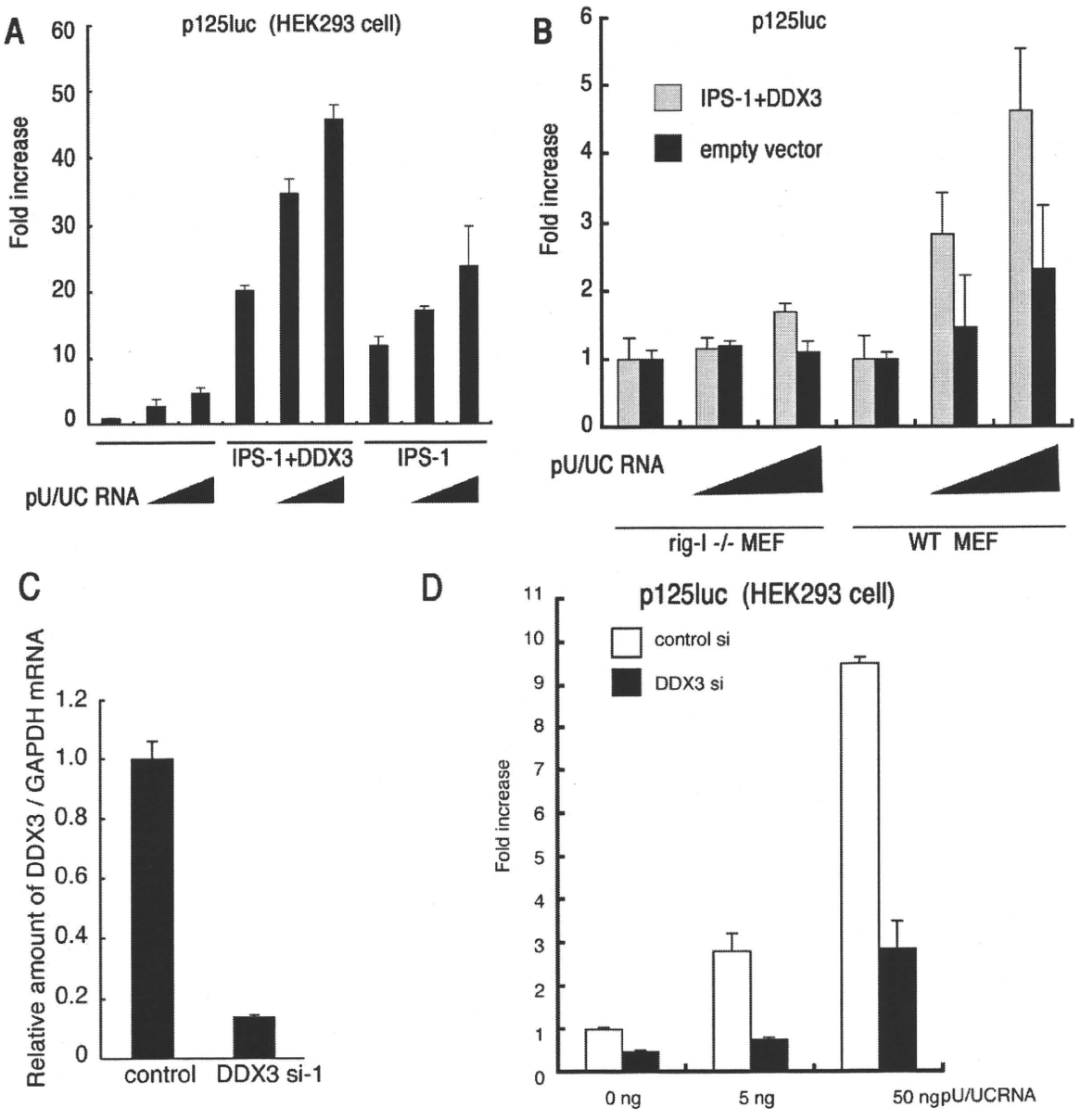

Figure 2. DDX3 is a positive regulator of IPS-1-mediated IFN promoter activation. (A) IFN-β induction by polyU/UC is augmented by DDX3. IPS-1 (100 ng), DDX3 (100 ng) and p125luc reporter (100 ng) plasmids were transfected into HEK293 cells in 24-well plates with or without the HCV 3′ UTR poly U/UC region (PU/UC) RNA (0, 25 or 50 ng/well), synthesized *in vitro* by T7 RNA polymerase. HCV RNA-enhancing activation of IFN-beta promoter was assessed by reporter assay in the presence or absence of the DDX3-IPS-1 complex. (B) RIG-I is essential for the DDX3/IPS-1-mediated IFN-promoter activation. MEF from wild-type and RIG-I −/− mice were transfected with plasmids of IPS-1, DDX3 and p125luc as in panel A, and stimulated with polyU/UC (0, 25 or 50 ng/well). Reporter activity was determined as in panel A. (C) Knockdown of DDX3. Negative control or DDX3 targeting siRNA (20 pmol), DDX3 si-1, was transfected into HEK293 cells, and after 48 hrs, expression of endogenous DDX3 mRNA was examined by real-time RT-PCR. DDX3 si-1-mediated down-regulation of the DDX3 protein was also confirmed by Western blotting (data not shown). (D) DDX3 enhances RIG-I-mediated IFN-beta promoter activation induced by polyU/UC. DDX3 si-1 or control siRNA was transfected into HEK293 cells with reporter plasmids (100 ng). After 48 hrs, cells were stimulated with polyU/UC (5~50 ng/ml) with lipofectamin 2000 reagent for 6 hrs, and activation of the reporter p125luc was measured. The results are representative of at least two independent experiments, each performed in triplicate.
doi:10.1371/journal.pone.0014258.g002

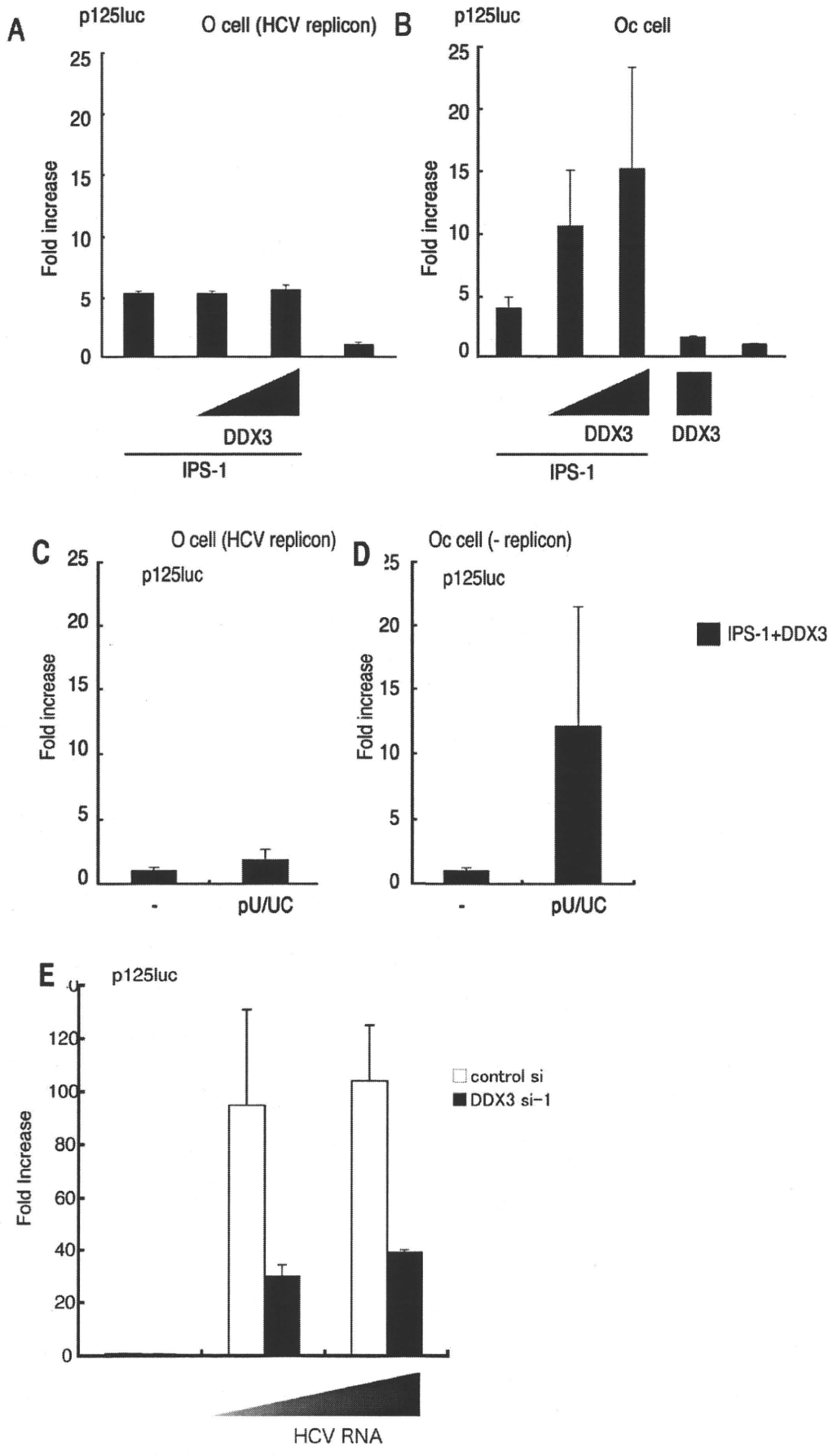
A
p125luc
O cell (HCV replicon)
Fold increase
25
20
15
10
5
0
DDX3
IPS-1
B
p125luc
Oc cell
Fold increase
25
20
15
10
5
0
DDX3
DDX3
IPS-1
C
O cell (HCV replicon)
p125luc
Fold increase
25
20
15
10
5
0
-
pU/UC
D
Oc cell (- replicon)
p125luc
Fold increase
25
20
15
10
5
0
-
pU/UC
IPS-1+DDX3
E
p125luc
Fold Increase
120
100
80
60
40
20
0
control si
DDX3 si-1
HCV RNA

Figure 3. The HCV replicon suppresses IPS-1/DDX3-mediated augmentation of IFN promoter activation. (A,B) O cells with the HCV replicon fail to activate an IFN-β reporter in response to IPS-1/DDX3. O cells contain the full-length HCV replicon, and Oc cells do not [16]. O cells (A) or Oc cells (B) were transfected with IPS-1, DDX3 or p125luc reporter plasmids. At timed intervals (24 hrs), reporter activity was determined as in Fig. 2. (C,D) The HCV replicon suppresses IFN-promoter activation by polyU/UC. O cells and Oc cells expressing IPS-1 and DDX3 were stimulated with polyU/UC. At 48 hrs, reporter activity was determined as in panel A. (E) DDX3 is required for enhanced activation of IFN-beta promoter by O cell HCV 3′UTR. HCV 3′ UTR cDNA was amplified by RT-PCR from RNA extracted from O cells containing full-length HCV replicon. The HCV 3′ UTR RNA was synthesized *in vitro* using T7 RNA polymerase. DDX3 siRNA or control siRNA was transfected into HEK293 cells with the p125luc reporter. After 24 hrs, cells were transfected with HCV RNA, and incubated for 24 hrs. The IFN-beta promoter activation was assessed by luciferase reporter assay. One representative of at least three independent experiments, each performed in triplicate, is shown.
doi:10.1371/journal.pone.0014258.g003

Preparation of HCV polyU/UC RNA

The HCV genotype 1b polyU/UC RNA (from 9421 to 9480, Accession number: EU867431) [23] was synthesized by T7 RNA polymerase *in vitro*. The template dsDNA sequences were; Forward: TAA TAC GAC TCA CTA TAG GGT TCC CTT TTT TTT TTT CTT TTT TTT TTT TTT TTT TTT TTT TTT TTT CTC CTT TTT TTT TC, Reverse: GAA AAA AAA AGG AGA AAA AAA AAA AAA AAA AAA AAA AAA AGA AAA AAA AAA AGG GAA CCC TAT AGT GAG TCG TAT TA. The synthesized RNA was purified by TRIZOL reagent (Invitrogen). cDNA of HCV 3′ UTR region was amplified from total RNA of O cells using primers HCV-F1 and HCV-R1, and then cloned into pGEM-T easy vector. The primer set sequences were HCV-F1: CTC CAG GTG AGA TCA ATA GG and HCV-R1: CGT GAC TAG GGC TAA GAT GG. RNA was synthesized using T7 and SP6 RNA polymerases. Template DNA was digested by DNase I, and RNA was purified using TRIZOL (Invitrogen) according to manufacturer's instructions.

RNAi

Knockdown of DDX3 was carried out using siRNA, DDX3 siRNA-1: 5′-GAU UCG UAG AAU AGU CGA ACA-3′, siRNA-2: 5′-GGA GUG AUU ACG AUG GCA UUG-3′, siRNA-3: 5′-GCC UCA GAU UCG UAG AAU AGU-3′ and control siRNA: 5′-GGG AAG AUC GGG UUA GAC UUC-3′. 20 pmol of each siRNA was transfected into HEK293 cells in 24-well plate with Lipofectamin 2000 according to manufacture's protocol. Knockdown of DDX3 was confirmed 48 hrs after siRNA transfection. Experiments were repeated twice for confirmation of the results.

Reporter assay

HEK293 cells (4×10^4 cells/well) cultured in 24-well plates were transfected with the expression vectors for IPS-1, DDX3 or empty vector together with the reporter plasmid (100 ng/well) and an internal control vector, phRL-TK (Promega) (2.5 ng/well) using FuGENE (Roche) as described previously [23]. The p-125 luc reporter containing the human IFN-beta promoter region (−125 to +19) was provided by Dr. T. Taniguchi (University of Tokyo, Tokyo, Japan). The total amount of DNA (500 ng/well) was kept constant by adding empty vector. After 24 hrs, cells were lysed in lysis buffer (Promega), and the *Firefly* and *Renella* luciferase activities were determined using a dual-luciferase reporter assay kit (Promega). The *Firefly* luciferase activity was normalized by *Renella* luciferase activity and is expressed as the fold stimulation relative to the activity in vector-transfected cells. Experiments were performed three times in duplicate (otherwise indicated in the legends).

PolyI:C or polyU/UC stimulation

PolyI:C was purchased from GE Healthcare company, and solved in milliQ water. For polyI:C treatment, polyI:C was mixed with DEAE-dextran (0.5 mg/ml) (Sigma) in the culture medium, and the cell culture supernatant was replaced with the medium containing polyI:C and DEAE-dextran. Using DEAE-dextran, polyI:C is incorporated into the cytoplasm to activate RIG-I/MDA5.

HCV 3′ UTR poly U/UC region (PU/UC) RNA (0∼50 ng/well), which is synthesized *in vitro* by T7 RNA polymerase, transfected into HEK293 cells in 24-well plate by lipofectamin 2000 (Invitrogen) with other plasmids. Cells were allowed to stand for 24∼48 hrs and HCV RNA-enhancing activation of IFN-beta promoter was assessed by reporter assay.

Immunoprecipitation (i.p.)

HEK293FT cells were transfected in a 6-well plate with plasmids encoding DDX3, IPS-1, RIG-I or MDA5 as indicated in the figures. 24 hrs after tranfection, the total cell lysate was prepared by lysis buffer (20 mM Tris-HCl [pH 7.5] containing 125 mM NaCl, 1 mM EDTA, 10% Glycerol, 1% NP-40, 30 mM NaF, 5 mM Na_3Vo_4, 20 mM IAA and 2 mM PMSF), and the protein was immunoprecipitated with anti-HA polyclonal (SIGMA) or anti-FLAG M2 monoclonal Ab (SIGMA). The precipitated samples were resolved on SDS-PAGE, blotted onto a nitrocellulose sheet and stained with anti-HA (HA1.1) monoclonal (SIGMA), anti-HA polyclonal or anti-FLAG M2 monoclonal Ab.

Pull-down assay

The pull-down assay was performed according to the method described in Saito T et al. [24]. Briefly, the RNA used for the assay was purchased from JBioS, Co. Ltd (Saitama, Japan). The RNA sequences are (sense strand) AAA CUG AAA GGG AGA AGU GAA AGU G, (antisense strand)CAC UUU CAC UUC UCC CUU UCA GUU U. The biotin is conjugated at U residue at the 3′ end of antisence strand (underlined). Biotinylated double-stranded (ds)RNA were incubated for 1 hr at 25°C with 10 μg of protein from the cytoplasmic fraction of cells that were transfected with Flag-tagged RIG-I and HA-tagged DDX3 expressing vectors. The mixture was transferred into 400 μl of lysis buffer containing 25 μl of streptavidine Sepharose beads, rocked at 4°C for 2 h, collected by centrifugation, washed three times, resuspended in SDS sample buffer.

Proteome analysis of RNA-binding proteins

RNA-binding proteins were identified by affinity chromatography and Mass spectrometry. Briefly, cell lysate was prepared from human HEK293 or Raji cells as will be described elsewhere (Watanabe and Matsumoto, manuscript submitted for publication). The lysate was first applied to polyU-Sepharose and then the pass-through fraction was applied to PolyI:C-Sepharose. The eluted proteins were analyzed on Mass spectrometry using the MASCOT software.

Confocal analysis

HCV replicon-positive (O) or –negative (Oc) cells were plated onto cover glass in a 24-well plate. In the following day, cells were transfected with indicated plasmids using Fugene HD (Roch). The

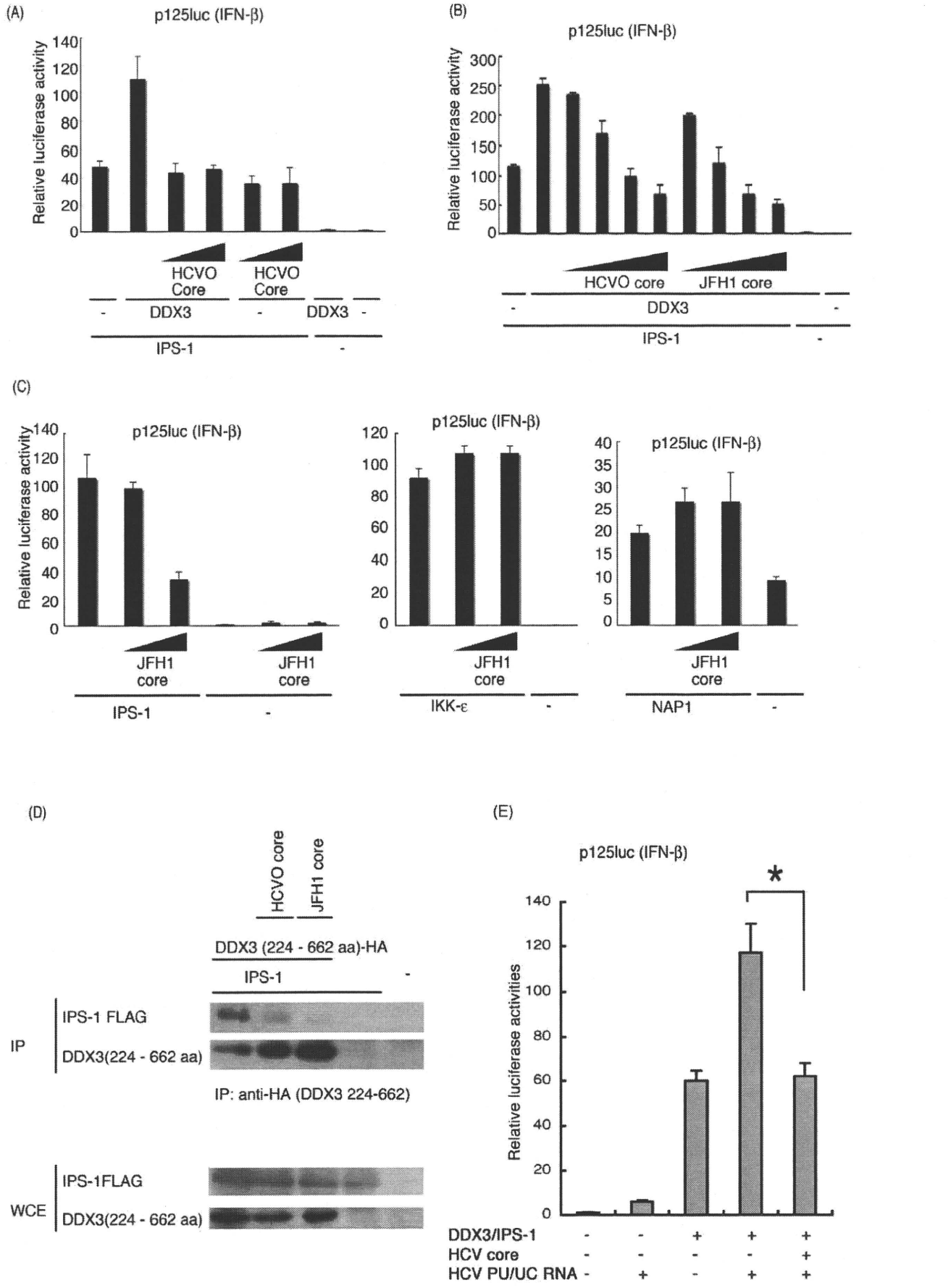
(A)
p125luc (IFN-β)
Relative luciferase activity
140
120
100
80
60
40
20
0
HCVO Core
HCVO Core
-
DDX3
-
DDX3
-
IPS-1
-
(B)
p125luc (IFN-β)
Relative luciferase activity
300
250
200
150
100
50
0
HCVO core
JFH1 core
-
DDX3
-
IPS-1
-
(C)
p125luc (IFN-β)
Relative luciferase activity
140
120
100
80
60
40
20
0
JFH1 core
JFH1 core
IPS-1
-
p125luc (IFN-β)
120
100
80
60
40
20
0
JFH1 core
IKK-ε
-
p125luc (IFN-β)
40
35
30
25
20
15
10
5
0
JFH1 core
NAP1
-
(D)
HCVO core
JFH1 core
DDX3 (224 - 662 aa)-HA
IPS-1
-
IP
IPS-1 FLAG
DDX3(224 - 662 aa)
IP: anti-HA (DDX3 224-662)
WCE
IPS-1FLAG
DDX3(224 - 662 aa)
(E)
p125luc (IFN-β)
*
Relative luciferase activities
140
120
100
80
60
40
20
0
DDX3/IPS-1 - - + + +
HCV core - - - - +
HCV PU/UC RNA - + - + +

Figure 4. HCV core protein inhibits DDX3 promotion of IPS-1-mediated IFN-beta induction. (A) Expression plasmids for IPS-1 (100 ng), DDX3 (200 ng) and/or HCVO core (50 or 100 ng) were transfected into HEK293 cells in 24-well plates with reporter plasmids, and reporter activity was examined. (B) Expression plasmids for IPS-1 (100 ng), DDX3 (100 ng), and/or HCVO or JFH1 core (10, 25, 50 or 100 ng) were transfected into HEK293 cells, and reporter gene expression was analyzed. (C) IPS-1-, IKKepsilon- or NAP1-expressing plasmids were transfected into HEK293 cells with HCV JFH1 core-expressing plasmids (25 or 100 ng), for reporter gene analysis. (D) Plasmids for expression of FLAG-tagged IPS-1 (400 ng), HA-tagged DDX3 partial fragment (400 ng) and HCVO or JFH1 core (400 ng) were transfected into HEK293FT cells. 24 hrs later cells were lyzed and the lysate was incubated with anti-HA Ab for immunoprecipitation. The DDX3 (224-662)-bound IPS-1 was blotted onto a sheet and probed with anti-Flag Ab. Whole cell lysate was also stained with anti-tag Abs. (E) IPS-1 (100 ng), DDX3 (100 ng), JFH1 core (50 ng) and/or p125 luc reporter (100 ng) plasmids were transfected with HEK293 cells, with HCV 3′UTR poly-U/UC (PU/UC) RNA (25 ng), synthesized *in vitro*. Cell lysates were prepared after 24 hrs, and luciferase activities measured. One representative of at least three independent experiments is shown except for panel D, which is a representative of two sets of the experiments.
doi:10.1371/journal.pone.0014258.g004

amount of DNA was kept constant by adding empty vector. After 24 hrs, cells were fixed with 3% of paraformaldehyde in PBS for 30 minutes, and then permeabilized with PBS containing 0.2% of Triton X-100 for 15 min. Permeabilized cells were blocked with PBS containing 1% BSA, and were labeled with anti-Flag M2 mAb (Sigma) or anti-HA pAb (Sigma) in 1% BSA/PBS for 1 hr at room temperature [25]. In some cases, endogenous proteins were directly stained with anti-core (C7-50) mAb (Affinity BioReagents, Inc) or anti-DDX3 pAbs (Abcam, Cambridge MA). The cells were then washed with 1% BSA/PBS and treated for 30 min at room temperature with Alexa-conjugated antibodies (Molecular Probes). Thereafter, micro-cover glass was mounted onto slide glass using PBS containing 2.3% DABCO and 50% of glycerol. The stained cells were visualized at ×60 magnification under a FLUOVIEW (Olympus, Tokyo, Japan).

Results

DDX3 binds RNA species

We have performed proteome analyses of RNA-binding fractions in human dendritic cell lysate eluted from polyU and polyI:C Sepharose. 127 cytoplasmic proteins were reproducibly identified as polyI:C-binding proteins (Watanabe and Matsumoto, unpublished data). Four of them are DEAD/H box helicases. In this setting, we found DDX3 is a RNA-binding protein (Fig. 1A). DDX3 in cell lysate bound both polyU and polyI:C, while the control PKR bound only to polyI:C.

Using biotinylayed dsRNA, RNA-binding properties of DDX3 and RIG-I were tested by pull-down assay. DDX3 or RIG-I protein was co-precipitated with dsRNA in HEK293 cells expressing either alone of DDX3 or RIG-I (Fig. 1B). Strikingly, higher amounts of DDX3 and RIG-I were precipitated with dsRNA in cells expressing both proteins (Fig. 1B). This, taken together with previous results [11,14,16], indicates that DDX3 assembles in some RNA, RIG-I, IPS-1 and HCV core protein in its C-terminal domain (Fig. S1).

PolyU/UC but not replicon enhances IFN-β induction via IPS-1/DDX3

A polyU/UC sequence is present in the 3′-region of the HCV genome, and serves as a ligand for RIG-I in IPS-1 pathway activation [23]. We produced the polyU/UC RNA and tested its IFN-beta-inducing activity in the presence or absence of DDX3 and IPS-1 (Fig. 2A). HCV polyU/UC promoted IPS-1-mediated IFN-beta induction, and this was further enhanced by forced expression of DDX3/IPS-1 (Fig. 2A). Similar results were obtained with wild-type mouse embryonic fibroblasts (MEF) (Fig. 2B). We also investigated whether DDX3 enhanced IPS-1-mediated IFN-β promoter activation in a RIG-I −/− MEF background (Fig. 2B). In IPS-1/DDX3-expressing MEF cells, polyU/UC IFN-induction was almost totally abrogated by the lack of RIG-I, suggesting that the trace RIG-I protein in the IPS-1 complex is required for DDX3 enhancement of the polyU/UC-mediated IFN response.

DDX3 mRNA (Fig. 2C) and protein [11] were depleted in HEK293 cells by gene silencing with si-1 siRNA, so this was used for DDX3 loss-of-function analysis. Control or DDX3-silinced cells were transfected with increasing amounts of polyU/UC and IFN-beta promoter activation was determined by luciferase assay. DDX3 loss-of-function resulted in a decrease of promoter activation by intrinsic polyU/UC (Fig. 2D). The result was confirmed with cells over-expressing RIG-I and exogenous polyI:C stimulation. HEK293 cells were transfected with a plasmid for the expression of RIG-I and stimulated with polyI:C, an activator of the IPS-1 pathway (Fig. S2A). IFN-beta reporter activation was suppressed in si-1-treated cells that expressed RIG-I, since polyI:C lots often contain short size duplexes that can activate RIG-I [26]. In addition, DDX3 augmented the IFN-beta response in cells expressing MDA5/IPS-1 (Fig. S2B). Thus, DDX3 was also crucial for IPS-1-mediated IFN-beta promoter activation.

We next determined whether the HCV replicon triggers IPS-1/DDX3 IFN promoter activation, using human hepatocyte lines with the HCV replicon (O cells) or without it (Oc cells). In O cells with the HCV replicon, IPS-1/DDX3 expression showed minimal enhancement of IFN-beta promoter activation (Fig. 3A), while in control Oc cells with no replicon, DDX3 facilitated IFN-beta promoter activation (Fig. 3B). Similarily, an augmented IFN promoter response to polyU/UC was observed in control Oc cells, but not in O cells (Figs. 3C and 3D). HCV RNA was prepared from O cells, and its ability to activate the IFN-beta reporter was tested in HEK293 cells (Fig. 3E). The HCV RNA of O cells had a high potency to induce reporter activation, and this activity was largely abrogated by si-1 siRNA treatment. Therefore, DDX3 augments IPS-1-mediated IFN-beta promoter activation in hepatocyte O cells, and HCV RNA, presumably the 3′UTR, participates in this induction. However, no IFN-beta reporter activation was detected in O cells which harbor HCV replicon. Therefore, an unidentified viral factor appeared to participate in suppressing virus RNA-mediated IFN-beta induction, which occurred in O cells overexpressing DDX3/IPS-1.

HCV core protein inhibits IPS-1 signaling through DDX3

What HCV proteins participate in IFN-beta induction was tested in a pilot study using protein expression analysis. We found that expression of HCV core protein as well as NS3/4A led to suppression of IFN-beta reporter activity in Oc cells (data not shown). The HCV core protein physically binds DDX3 [14,16], and co-localizes with DDX3 in the cytoplasm of HeLa cells transfected with HCV core protein [14]. Furthermore, we showed that DDX3 binds IPS-1, which resides on the mitochondrial outer membrane, and assembles into RNA-sensing receptors. Since some populations of the HCV core protein localize on the mitochondrial outer membrane [27], we tested if HCV core

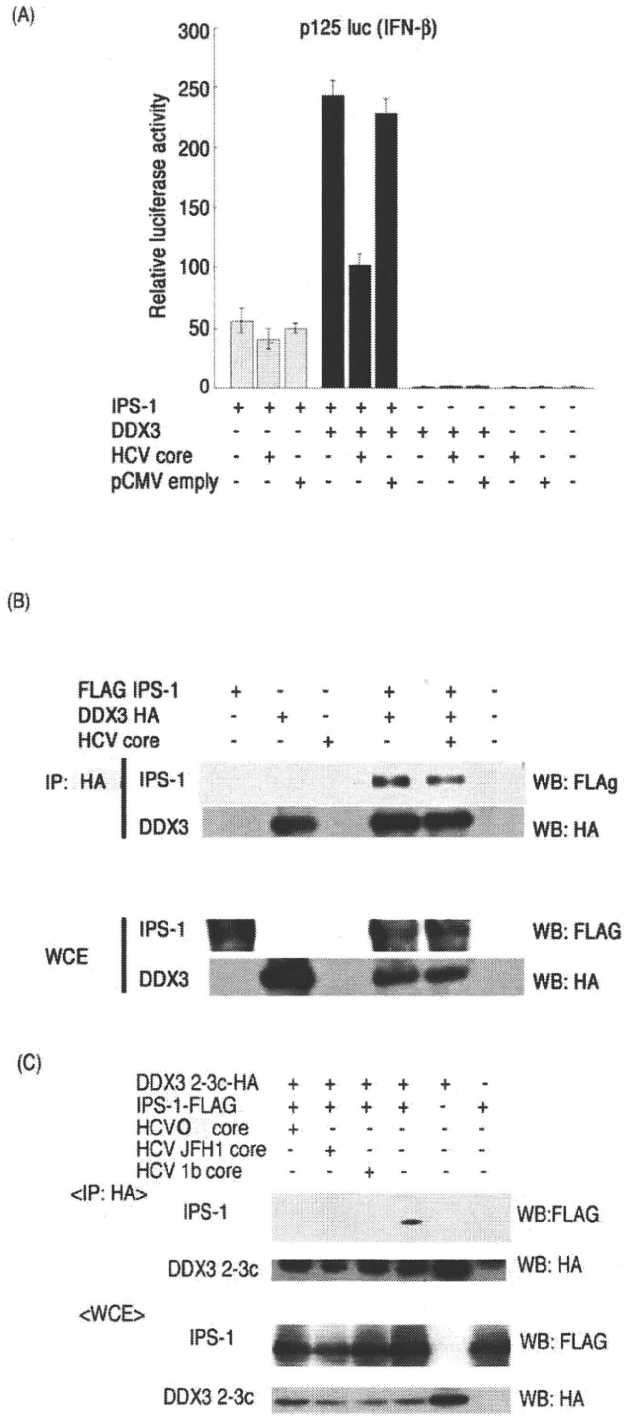

Figure 5. Properties of a 1b-type core protein in the IPS-1 pathway. (A) A core protein derived from an HCV patient suppressed DDX3-mediated activation of IPS-1 signaling. The 1b-type core protein was cloned into the pCMV vector from a patient with hepatitis C. IPS-1 (100 ng), DDX3 (100 ng) and HCV core (100 ng) expression vectors were transfected into HEK293 cells with a reporter plasmid (p125luc), for analysis as in Figure 4. (B) The core protein reduced interaction between full-length DDX3 and IPS-1. The plasmids encoding core protein (400 ng), DDX3-HA (400 ng) and FLAG-IPS-1 (400 ng) were transfected into HEK293FT cells. After 24 hrs, cell lysates were prepared and immunoprecipitation was carried out using anti-HA (DDX3-HA). (C) The core protein blocked interaction between the C-terminal fragment of DDX3 and IPS-1. The C-terminal region of DDX3 (199–662 aa) called DDX3 2-3c, IPS-1, HCV (O) and JFH1 or 1b core expression plasmids were transfected into HEK293FT cells. After 24 hrs, cell lysates were prepared and immunoprecipitation was carried out with anti-HA (DDX3 2–3c). Immunoprecipitates were analyzed by SDS-PAGE and Western blotting with anti-HA or FLAG antibodies. The results are representative of two independent experiments.
doi:10.1371/journal.pone.0014258.g005

protein affects IPS-1 signaling by binding to DDX3. The cDNAs for HCV core proteins, genotype 1b (HCVO) and 2a (JFH1) [16], were co-transfected into HEK293 together with IPS-1, DDX3, and reporter plasmids, and core protein interference with IPS-1/DDX3-mediated IFN-beta promoter activation was examined. We found that the core proteins of HCVO and JFH1 suppressed IPS-1/DDX3-augmented IFN-beta-induction in a dose-dependent manner (Fig. 4A and 4B). Without DDX3 transfection, core protein had no effect on IPS-1-mediated IFN-beta promoter activation (Fig. 4A). JFH1 core slightly more efficiently inhibited IPS-1/DDX3-augmented IFN-beta-induction than HCVO core (Fig. 4B).

Although some endogenous DDX3 was present in the cytoplasm without DDX3 transfection, only IPS-1 transfection permitted minimal induction of IFN-beta. It is notable that high doses of the HCV JFH1 core protein was needed to inhibit the IPS-1-mediated IFN-beta-induction signal (Fig. 4C, left panel). Since the imaging profile of DDX3 is not always monotonous in human cells, its distribution may be biased in the cytoplasm, which may reason that only a high dose of HCV core involves preoccupied DDX3 protein to inhibit the IPS-1 pathway. This is consistent with earlier reports on an NS3-independent mechanism to block IFN induction using HCV-infected Huh 7 cells [28].

IPS-1 transduces a RNA replication signal to result in IFN-beta output using downstream proteins, such as NAP1 and IKKeysilon. If the HCV core protein interferes with IPS-1 function through DDX3, the core should not inhibit over-expressed downstream molecules. As predicted, HCV core protein did not suppress the IKKepsilon- or NAP1-mediated IFN-beta-inducing signal (Fig. 4C, center and right panels). Hence, the core protein blocks the action of endogenous DDX3 and overexpressed IPS-1 to facilitate minimal IFN-beta promoter activation, and this IFN-beta blocking function of core does not target IKKepsilon or NAP1 (Fig. 4C). An upstream molecule of IKKepsilon and NAP1 is predicted to be the target of the HCV core protein, which is in line with the fact that the HCV core protein interacts with DDX3 [14,16].

To further confirm this model, we examined whether the HCV core protein inhibits the physical interaction between IPS-1 and DDX3. Full length IPS-1 and the C-terminal fragment of DDX3, which binds to the IPS-1 CARD-like region, were transfected into HEK293 cells, with or without the HCV core protein, and the DDX3 fragment was immunoprecipitated. Expression of HCV core proteins strongly inhibited interaction between the DDX3 C-terminal fragment and IPS-1 (Fig. 4D). JFH1 core appeared to show greater inhibition to DDX3-IPS-1 interaction than HCVO. We then examined this IFN-beta blocking function of JFH1 core in a similar cell condition plus polyU/UC. DDX3/IPS-1-enhanced p125luc reporter activity in cells stimulated with polyU/UC (Fig. 4E) was decreased in cells expressing HCV core. The results suggest that the role of the core in HCV-infected cells is to remove DDX3 from IPS-1, and facilitate its interaction with HCV replication complex (Fig. S1).

PolyU/UC HCV RNA activates the IFN-beta promoter (Fig. 2A), and this activity was inhibited by expression of the HCV core protein (Fig. 4E). PolyI:C/RIG-I-mediated IFN-β promoter activation was similarly suppressed by the core protein

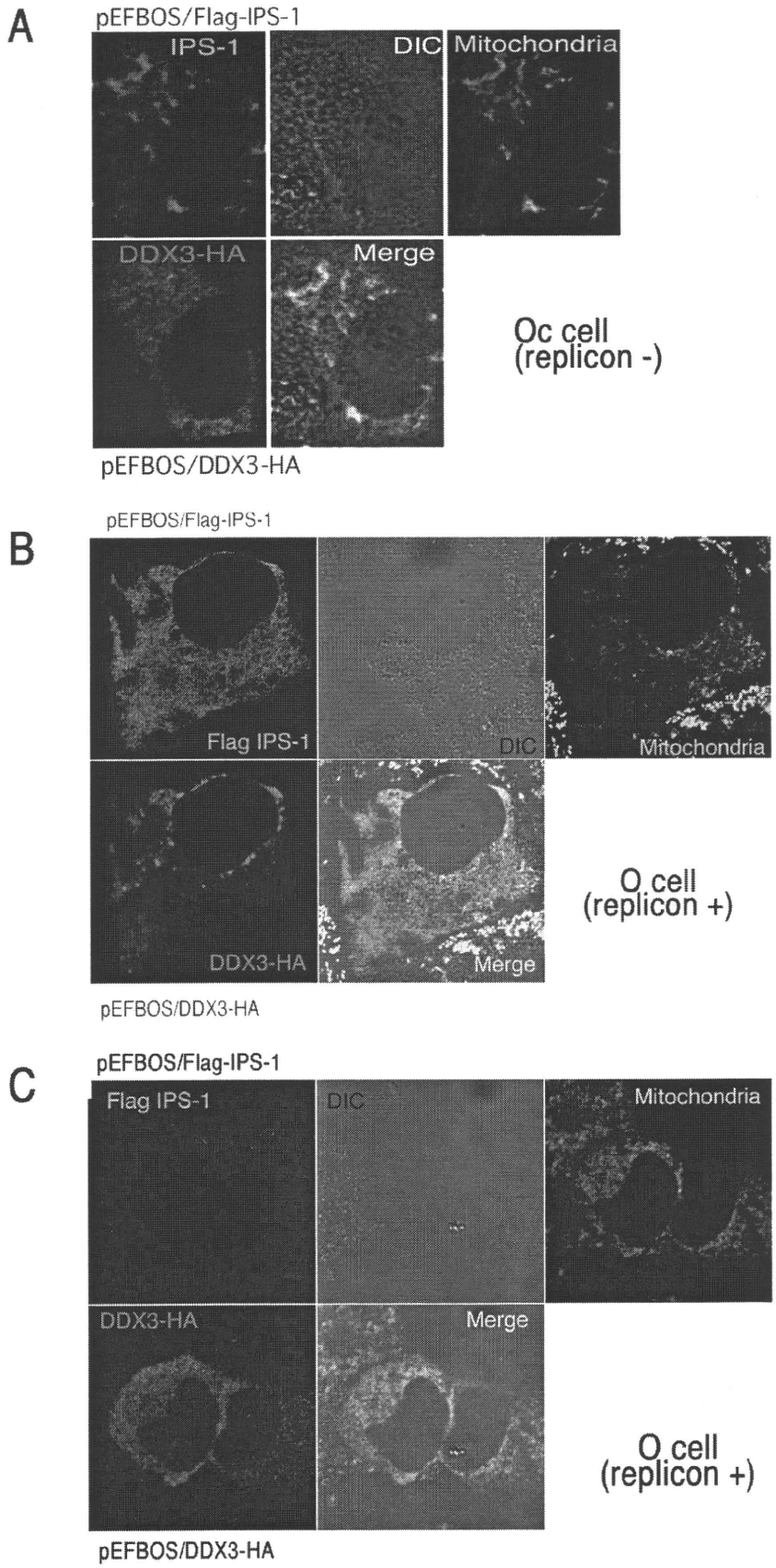
A
pEFBOS/Flag-IPS-1
IPS-1
DIC
Mitochondria
DDX3-HA
Merge
Oc cell
(replicon -)
pEFBOS/DDX3-HA
B
pEFBOS/Flag-IPS-1
Flag IPS-1
DIC
Mitochondria
DDX3-HA
Merge
O cell
(replicon +)
pEFBOS/DDX3-HA
C
pEFBOS/Flag-IPS-1
Flag IPS-1
DIC
Mitochondria
DDX3-HA
Merge
O cell
(replicon +)
pEFBOS/DDX3-HA

Figure 6. Distribution of DDX3 and IPS-1. (A) DDX3 colocalizes with IPS-1 on the mitochondria in Oc cells. HA-tagged DDX3 and FLAG-tagged IPS-1 were co-transfected into Oc cells. After 24 hrs, cells were fixed with formaldehyde and stained with anti-HA polyclonal and FLAG monoclonal Abs. Alexa488 (DDX3-HA) or Alexa633 antibody was used for second antibody. Mitochondria were stained with Mitotracker Red. Similar IPS-1-DDX3 merging profiles were observed in Huh7.5.1 cells (Fig. S3). (B,C) O cells with the HCV replicon poorly formed the DDX3-IPS-1 complex. Plasmids carrying IPS-1 (100 ng) or DDX3 (150 or 300 ng) were transfected into O (HCV replicon +) as in Oc cells (no replicon, panel A). After 24 hrs, localization of IPS-1 and DDX3 was examined by confocal microscopy. Two representatives which differ from the conventional profile (as in panel A) are shown. Similar sets of experiments were performed four times to confirm the results.
doi:10.1371/journal.pone.0014258.g006

(Fig. S2A). MDA5-dependent IFN-beta promoter activation was also suppressed by the core expression (Fig. S2B). The inhibitory effect of the core protein on DDX3-IPS-1 interaction was further confirmed using an 1b core isoform isolated from a patient. This HCV core protein also reduced interaction as well as IPS-1-mediated IFN-beta promoter activation (Fig. 5A). The blocking effect was relatively weak in cells expressing IPS-1 and full-length DDX3 (Fig. 5B). We presume that this is because there are multiple binding sites for IPS-1 in the DDX3 whole molecule [11]. For binding assay, we used DDX3 2-3c (across a.a. 199~662, longer than 224~662) instead of the whole DDX3. In fact, DDX3(199-662)-IPS-1 interaction was blocked by the additional expression of core protein (HCVO, JFH1 or 1b core) in Fig. 5C. Ultimately, HCV core protein suppresses IPS-1 signaling by blocking the interaction between the C-terminal region of DDX3 and the CARD-like region of IPS-1, and this inhibition apparently causes the disruption of the active RIG-I/DDX3/IPS-1 complex that efficiently induces IFN-beta production signaling.

Localization of DDX3 and HCV core protein in O cells

We attempted to confirm this finding by tag-expressed proteins and imaging analysis. In Huh7.5 cells IPS-1 colocalized with DDX3 around the mitochondria (Fig. S3), and so did in the hepatocyte lines Oc cells with no HCV replicon (Fig. 6A). In Oc and Huh7.5.1 cells with no HCV replicon, abnormal distribution of IPS-1 was barely observed (Fig. 6A, Fig. S3). In O cells expressing DDX3 and IPS-1, by contrast, two distinct profiles of IPS-1 were observed in addition to the Fig. 6A pattern of IPS-1: diminution or spreading of the IPS-1 protein over mitochondria (Fig. 6B,C). IPS-1 may be degraded by NS3/4A in some replicon-expressing O cells as reported previously [5,28]. We counted number of cells having the pattern represented by Fig. 6 panel B and those similar to Fig. 6 panel C, and in most cases the latter patterns were predominant.

What happens in the O cells with replicon when the core protein is expressed was next tested. Using O and Oc cells, we tested the localization of the core protein and DDX3 in comparison with IFN-inducing properties (Fig. 3). In O cells with full-length HCV replicon, DDX3 was localized proximal to the lipid droplets (LD) (Fig. 7A top panel) around which HCV particles assembled [29]. HCV core protein and DDX3 were partly colocalized in the HCV replicon-expressing cells (Fig. 7A center panel). The results were confirmed with HCV replicon-expressing O cells where endogenous core and DDX3 were stained (Fig. 7B upper panel). Partial merging between core and DDX3 was reproduced in this case, too. In contrast, sO cells, which possess a subgenomic replicon lacking the cording region of the core protein, showed no merging profile of DDX3 and LD (Fig. 7A bottom panel). Likewise, Oc cells barely formed assembly consisting of LD (where the core assembles) and overexpressed DDX3 (Fig. 7A bottom panel) or endogenous DDX3 (Fig. 7B lower panel). O cells expressing DDX3 tended to form large spots compared to Oc cells (with no replicon) and sO cells (core-less replicon) with DDX3.

Overexpressed DDX3 allowed the Oc cells to induce IPS-1-mediated IFN-beta promoter activation (Fig. 3B), while this failed to happen in O cells having HCV replicon (Fig. 3A). Ultimately, overexpressed IPS-1 did not facilitate efficient merging with DDX3 in O cells with replicon (Fig. 6B,C) compared to Oc cells or Huh7.5 cells with no replicon (Fig. 6A, Fig. S3). The results on the functional and immnoprecipitation analyses, together with the imaging profiles, infer that the IPS-1-enhancing function of DDX3 should be blocked by both NS3/4A-mediated IPS-1 degradation and the HCV core which translocates DDX3 from the IPS-1 complex to the proximity of LD in HCV replicon-expressing cells.

Discussion

We investigated the effect of the HCV core protein on the cytosolic DDX3 that forms a complex with IPS-1 to enhance the RIG-I-mediated RNA-sensing pathway. We demonstrated that the core protein removes DDX3 from the IFN-β-inducing complex, leading to suppression of IFN-β induction. DDX3 is functionally complex, since its protective role against viruses may be modulated by the synthesis of viral proteins. DDX3 acts on multiple steps in the IFN-inducing pathway [30]. In addition, DDX3 interacts with the HCV core protein in HCV-infected cells and promotes viral replication [16]. This alternative function is accelerated by the HCV core protein, resulting in augmented HCV propagation [14,16]. More recently, Patal et al., reported that interaction of DDX3 with core protein is not critical for the support of viral replication by DDX3, although DDX3 and core protein colocalize with lipid droplet [15]. If this is the case, what function is revealed by the interaction between DDX3 and HCV core protein remain unsettled. At least, HCV replication is not blocked by this molecular interaction [15].

It remains unclear in Fig. 4C why higher doses of JFH1 core protein are required to inhibit enhancement of IPS-1 signaling by endogenous DDX3 than by exogenously overexpressed DDX3. One possibility is that endogenous DDX3 is preoccupied in a molecular complex other than the IPS-1 pathway since DDX3 is involved in almost every step of RNA metabolism and its localization affects its functional profile [18,30].

Together with these findings, the results presented here suggest that the HCV core inactivates IPS-1 in a mode different from NS3/4A [5,31]. The core protein may switch DDX3 from an antiviral mode to an HCV propagation mode. The core protein localizes to the N-terminus of the HCV translation product, and is generated in infected cells before NS3/4A proteolytically liberates non-structural proteins and inactivates IPS-1. Our results on how the HCV core protein interferes with the interaction between DDX3 and IPS-1 add several possibilities to notions about the HCV function on the IFN-beta-inducing pathway [18].

DDX3 appears to be a prime target for viral manipulation, since at least three different viruses, including HCV [14], Hepatitis B virus [32], and poxviruses [8], encode proteins that interact with DDX3 and modulate its function. These viruses seem to co-opt DDX3, and also require it for replication. The viruses are all oncogenic, and may confer oncogenic properties to DDX3.

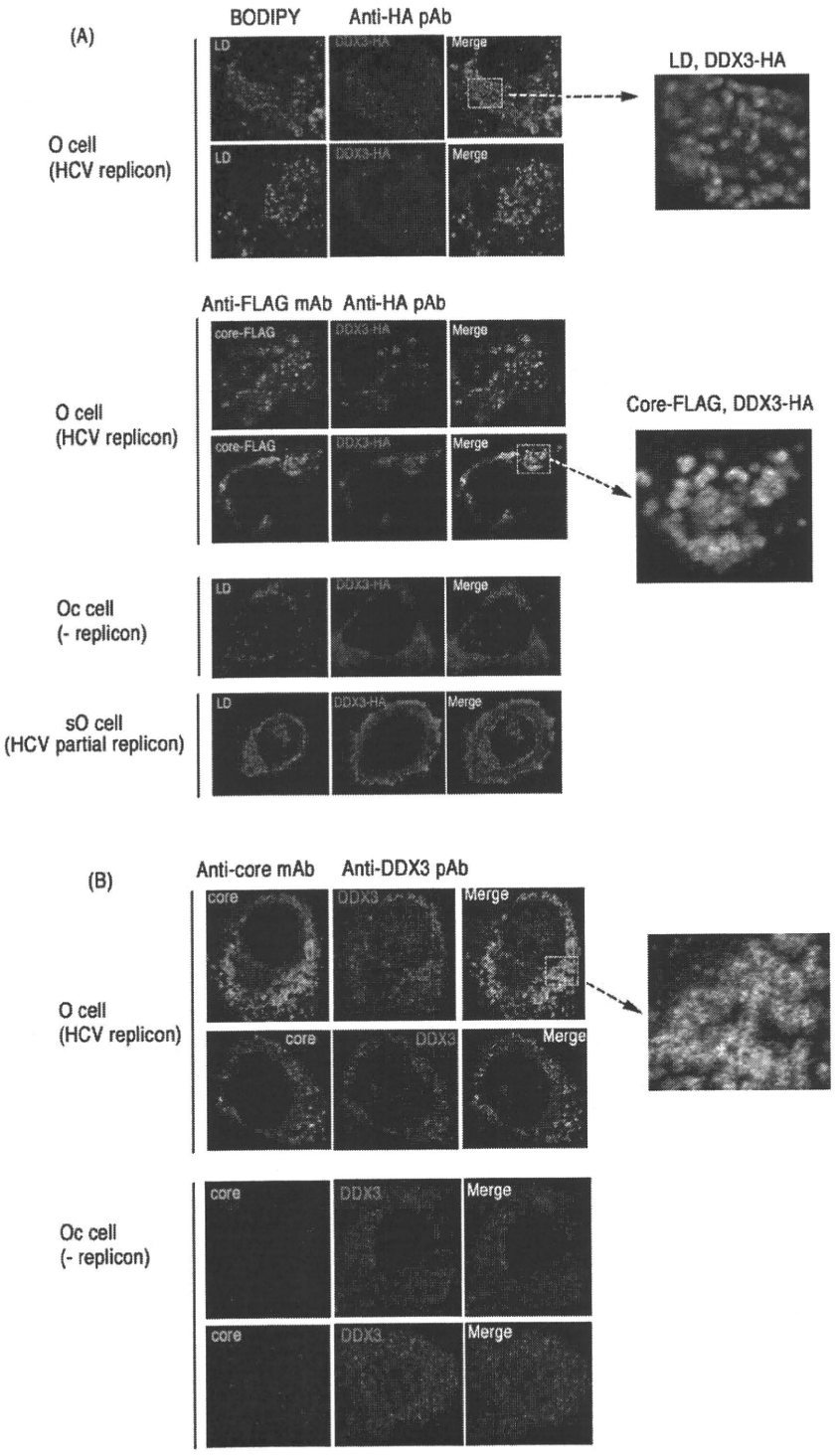

Figure 7. Partial association of endogenous and overexpressed DDX3 with HCV core protein in hepatocyte lines. (A) O cells with the HCV replicon form DDX3-containing speckles in the cytoplasm. O cells contain full-length HCV replicon, and Oc cells do not [16]. O cells were transfected with a plasmid expressing HA-tagged DDX3 (top panel). In other experiments, O cells were transfected with plasmids expressing HA-tagged DDX3 and FLAG-tagged HCV core protein (center panel). After 24 hrs, cells were stained with anti-HA or FLAG antibodies. Proteins were visualized with Alexa488 or 564 second antibodies and the LD was stained with BODIPY493/503. In the bottom panel, Oc cells (no replicon) and sO cells with the core-less subgenomic replicon [16] were transfected with a plasmid expressing HA-tagged DDX3. After 24 hrs, cells were stained with anti-HA antibodies. LD was stained with BODIPY493/503. (B) Endogenous DDX3-HCV core association in O cells. O or Oc cells were cultured to amplify the HCV replicon. Cells were stained with anti-core mAb and anti-DDX3pAb and secondary antibodies. Similar sets of experiments were performed three times to confirm the results.
doi:10.1371/journal.pone.0014258.g007

DDX3 is also involved in human immunodeficiency virus RNA translocation [33]. The DDX3 gene is conserved among eukaryotes, and includes the budding yeast homolog, Ded1 [34]. The Ded1 helicase is essential for initiation of host mRNA translation, and human DDX3 complements the lethality of Ded1 null yeast [14,35]. Another function of DDX3 is to bind viral RNA to modulate RNA replication and translocation. Constitutive expression of the HCV core or other DDX3-binding proteins may impede IFN induction and promote cell cycle progression. These reports are consistent with the implication of DDX3 in various steps of RNA metabolism in cells that contain both host and viral RNAs.

A continuing question is the physiological role of the molecular complex of DDX3 and IPS-1 during replication of HCV in hepatocytes. HCV proteins generated in host hepatocytes usually induce an HCV-permissive state in patients, for example in the IFN-inducing pathways. NS3/4A protease induces rapid degradation of IPS-1 [5,31] and TICAM-1/TRIF [36]. NS5A interferes with the MyD88 function [37]. Viral replication ultimately blocks the STAT1-mediated IFN-amplification pathway [38]. PKR may be an additional factor by which HCV controls type I IFN production [39]. Our results add to our knowledge of the mechanism of how HCV circumvents IFN induction in host cells: HCV core protein suppresses the initial step of IFN-beta induction by interfering with DDX3-IPS-1 association. Indeed, the core protein functions as the earliest IFN suppressor, since it is generated first in HCV-infected cells, and rapidly couples with DDX3 to retract it from the IPS-1 complex, resulting in localization of DDX3 near the LD (Fig. 7). It is HCV that hijacks this protein for establishing infection. Although gene disruption of DDX3 makes mice lethal, this issue will be further tested using IPS-1 −/− hepatocytes expressing human CD81 and occludin [40], in which HCV replication would proceed.

DDX3 primarily is an accelerating factor for antiviral response through IPS-1-binding. Many host proteins other than DDX3 may positively regulate HCV replication in hepatocytes in association with the IPS-1 pathway. In this context, we know LGP2 [41] and STING [42] act as positive regulators in virus infection. Peroxisomes serve as signaling platforms for recruiting IPS-1 with a different signalosome than mitochondria [43]. It appears rational that HCV harbors strategies to circumvent these positive regulators in the relevant steps of the IFN-inducing pathway.

Imaging studies suggest that the complex of IPS-1 involving the membrane of mitochondrial/peroxisomes differ from that free from the membrane. Although IPS-1 is liberated from the membrane by NS3/4A having largely intact cytosolic domain, it loses the IFN-inducing function [5,31]. Our results could offer the possibility that the clipped-out form of IPS-1 immediately fails to form the conventional complex for IRF-3 activation any more [44] or is easily degraded further to be inactive (Fig. 6C). Indeed, there are a number of mitochondria-specific molecules which assemble with IPS-1 [45]. Formation of the molecular complex on the mitochondria rather than simple association between IPS-1 and DDX3 may be critical for the DDX3 function.

Evidence is accumulating that HCV checks many steps in the IFN-inducing pathway throughout the early and late infection stages, and suppresses IFN production by multiple means. Disruption of IPS-1 function by both NS3/4A and core protein may be crucial in HCV-infected Huh7.5 cells, even though the cells harbor dysfunctional RIG-I [46]. Type I IFN suppresses tumors by causing expression of p53 and other tumor-suppressing agents [47]. These unique features of the HCV core protein require further confirmation, and should be minded in investigation of HCV persistency, chronic infection and progression to cirrhosis and carcinoma.

Supporting Information

Figure S1 The IPS-1 complex. IPS-1 and HCV core bind C-terminal regions of DDX3. DDX3 captures dsRNA at the C-terminal domain. This figure is constructed from [11], [14] and [16].
Found at: doi:10.1371/journal.pone.0014258.s001 (0.41 MB TIF)

Figure S2 DDX3 enhances RIG-I-mediated IFN-β promoter activation induced by polyI:C. (A) DDX3 si-1 or control siRNA was transfected into HEK293 cells with reporter plasmids and RIG-I-expression plasmid or control plasmid (100 ng). After 48 hrs, cells were stimulated with polyI:C (20 μg/ml) with dextran for 4 hrs, and activation of the reporter p125luc was measured. (B) MDA5 (25 ng), IPS-1 (100 ng), DDX3 (100 ng), JFH1 core (50 ng) and/or p125 luc reporter (100 ng) plasmids were transfected with HEK293 cells. Cell lysates were prepared after 24 hrs, and luciferase activities measured. The results are representative of two independent experiments, each performed in triplicate.
Found at: doi:10.1371/journal.pone.0014258.s002 (0.17 MB TIF)

Figure S3 DDX3 colocalizes with IPS-1 on the mitochondria in Huh7.5.1 cells. HA-tagged DDX3 and FLAG-tagged IPS-1 were co-transfected into Huh7.5.1 cells. After 24 hrs, cells were fixed with formaldehyde and stained with anti-HA polyclonal and FLAG monoclonal Abs. Alexa488 (DDX3-HA) or Alexa633 antibody was used for second antibody. Mitochondria were stained with Mitotracker Red. A representative result from three independent experiments is shown.
Found at: doi:10.1371/journal.pone.0014258.s003 (0.92 MB TIF)

Acknowledgments

We thank Drs. Y. Matsuura (Osaka Univ.), Kyoko Mori (Okayama Univ.), and M. Sasai (Yale Univ.) for invaluable discussions. Thanks are also due to Drs. T. Ebihara, K. Funami, A. Matsuo, A. Ishii, and M. Shingai in our laboratory for their critical discussions.

Author Contributions

Conceived and designed the experiments: HO MM TS. Performed the experiments: HO MM. Analyzed the data: HO MM KS TS. Contributed reagents/materials/analysis tools: MI AW OT SA NK KS. Wrote the paper: HO TS.

References

1. Yoneyama M, Kikuchi M, Natsukawa T, Shinobu N, Imaizumi T, et al. (2004) The RNA helicase RIG-I has an essential function in double-stranded RNA-induced innate antiviral responses. Nat Immunol 5: 730–737.
2. Yoneyama M, Kikuchi M, Matsumoto K, Imaizumi T, Miyagishi M, et al. (2005) Shared and unique functions of the DExD/H-box helicases RIG-I, MDA5, and LGP2 in antiviral innate immunity. J Immunol 175: 2851–2858.
3. Kato H, Takeuchi O, Sato S, Yoneyama M, Yamamoto M, et al. (2006) Differential roles of MDA5 and RIG-I helicases in the recognition of RNA viruses. Nature 441: 101–105.
4. Kawai T, Takahashi K, Sato S, Coban C, Kumar H, et al. (2005) IPS-1, an adaptor triggering RIG-I- and Mda5-mediated type I interferon induction. Nat Immunol 6: 981–988.

5. Meylan E, Curran J, Hofmann K, Moradpour D, Binder M, et al. (2005) Cardif is an adaptor protein in the RIG-I antiviral pathway and is targeted by hepatitis C virus. Nature 437: 1167–1172.
6. Seth RB, Sun L, Ea CK, Chen ZJ (2005) Identification and characterization of MAVS, a mitochondrial antiviral signaling protein that activates NF-kappaB and IRF 3. Cell 122: 669–682.
7. Xu LG, Wang YY, Han KJ, Li LY, Zhai Z, et al. (2005) VISA is an adapter protein required for virus-triggered IFN-beta signaling. Mol Cell 19: 727–740.
8. Schroder M, Baran M, Bowie AG (2008) Viral targeting of DEAD box protein 3 reveals its role in TBK1/IKKepsilon-mediated IRF activation. Embo J 27: 2147–2157.
9. Soulat D, Bürckstümmer T, Westermayer S, Goncalves A, Bauch A, et al. (2008) The DEAD-box helicase DDX3X is a critical component of the TANK-binding kinase 1-dependent innate immune response. Embo J 27: 2135–2146.
10. Kravchenko VV, Mathison JC, Schwamborn K, Mercurio F, Ulevitch RJ (2003) IKKi/IKKepsilon plays a key role in integrating signals induced by pro-inflammatory stimuli. J Biol Chem 278: 26612–26619.
11. Oshiumi H, Sakai K, Matsumoto M, Seya T (2010) DEAD/H BOX 3 (DDX3) helicase binds the RIG-I adaptor IPS-1 to up-regulate IFN-beta inducing potential. Eur J Immunol 40: 940–948.
12. Chao CH, Chen CM, Cheng PL, Shih JW, Tsou AP, et al. (2006) A DEAD box RNA helicase with tumor growth-suppressive property and transcriptional regulation activity of the p21wafl/cipl promoter, is a candidate tumor suppressor. Cancer Res 66: 6579–6588.
13. Rocak S, Linder P (2004) DEAD-box proteins: the driving forces behind RNA metabolism. Nat Rev Mol Cell Biol 5: 232–241.
14. Owsianka AM, Patel AH (1999) Hepatitis C virus core protein interacts with a human DEAD box protein DDX3. Virology 257: 330–340.
15. Angus AGN, Dalrymple D, Boulant S, McGivern DR, Clayton RF, et al. (2010) Requirement of cellular DDX3 for hepatitis C virus replication is unrelated to its interaction with the viral core protein. J Gen Virol 91: 122–132.
16. Ariumi Y, Kuroki M, Abe K, Dansako H, Ikeda M, et al. (2007) DDX3 DEAD-box RNA helicase is required for hepatitis C virus RNA replication. J Virol 81: 13922–13926.
17. Chang PC, Chi CW, Chau GY, Li FY, Tsai YH, et al. (2006) DDX3, a DEAD box RNA helicase, is deregulated in hepatitis virus-associated hepatocellular carcinoma and is involved in cell growth control. Oncogene 25: 1991–2003.
18. Schroder M (2010) Human DEAD-box protein 3 has multiple functions in gene regulation and cell cycle control and is a prime target for viral manipulation. Biochem Pharmacol 79: 297–306.
19. Ikeda M, Abe K, Dansako H, Nakamura T, Naka K, et al. (2005) Efficient replication of a full-length hepatitis C virus genome, strain O, in cell culture, and development of a luciferase reporter system. Biochem Biophys Res Commun 329: 1350–1359.
20. Lin W, Kim SS, Yeung E, Kamegaya Y, Blackard JT, et al. (2006) Hepatitis C virus core protein blocks interferon signaling by interaction with the STAT1 SH2 domain. J Virol 2006 Sep; 80(18): 9226–35.
21. Sasai M, Shingai M, Funami K, Yoneyama M, Fujita T, et al. (2006) NAK-associated protein 1 participates in both the TLR3 and the cytoplasmic pathways in type I IFN induction. J Immunol 177: 8676–8683.
22. Oshiumi H, Matsumoto M, Funami K, Akazawa T, Seya T (2003) TICAM-1, an adaptor molecule that participates in Toll-like receptor 3-mediated interferon-beta induction. Nat Immunol 4: 161–167.
23. Saito T, Owen DM, Jiang F, Marcotrigiano J, Gale M, Jr. (2008) Innate immunity induced by composition-dependent RIG-I recognition of hepatitis C virus RNA. Nature 454: 523–527.
24. Saito T, Hirai R, Loo YM, Owen D, Johnson CL, et al. (2007) Regulation of innate antiviral defenses through a shared repressor domain in RIG-I and LGP2. Proc Natl Acad Sci U S A 104: 582–587.
25. Matsumoto M, Funami K, Tanabe M, Oshiumi H, Shingai M, et al. (2003) Subcellular localization of Toll-like receptor 3 in human dendritic cells. J Immunol 171: 3154–3162.
26. Oshiumi H, Matsumoto M, Hatakeyama S, Seya T (2009) Riplet/RNF135, a RING finger protein, ubiquitinates RIG-I to promote interferon-beta induction during the early phase of viral infection. J Biol Chem 284: 807–817.
27. Schwer B, Ren S, Pietschmann T, Kartenbeck J, Kaehlcke K, et al. (2004) Targeting of hepatitis C virus core protein to mitochondria through a novel C-terminal localization motif. J Virol 78: 7958–7968.
28. Cheng G, Zhong J, Chisari FV (2006) Inhibition of dsRNA-induced signaling in hepatitis C virus-infected cells by NS3 protease-dependent and -independent mechanisms. Proc Natl Acad Sci U S A 103: 8499–8504.
29. Miyanari Y, Atsuzawa K, Usuda N, Watashi K, Hishiki T, et al. (2007) The lipid droplet is an important organelle for hepatitis C virus production. Nat Cell Biol 9: 1089–1097.
30. Mulhern O, Bowie AG (2010) Unexpected roles for DEAD-box protein 3 in viral RNA sensing pathways. Eur J Immunol 40: 933–935.
31. Li XD, Sun L, Seth RB, Pineda G, Chen ZJ (2005) Hepatitis C virus protease NS3/4A cleaves mitochondrial antiviral signaling protein off the mitochondria to evade innate immunity. Proc Natl Acad Sci U S A 102: 17717–17722.
32. Wang H, Kim S, Ryu WS (2009) DDX3 DEAD-Box RNA helicase inhibits hepatitis B virus reverse transcription by incorporation into nucleocapsids. J Virol 83: 5815–5824.
33. Yedavalli VS, Neuveut C, Chi YH, Kleiman L, Jeang KT (2004) Requirement of DDX3 DEAD box RNA helicase for HIV-1 Rev-RRE export function. Cell 119: 381–392.
34. Chuang RY, Weaver PL, Liu Z, Chang TH (1997) Requirement of the DEAD-Box protein ded1p for messenger RNA translation. Science 275: 1468–1471.
35. Mamiya N, Worman HJ (1999) Hepatitis C virus core protein binds to a DEAD box RNA helicase. J Biol Chem 274: 15751–15756.
36. Li K, Foy E, Ferreon JC, Nakamura M, Ferreon AC, et al. (2005) Immune evasion by hepatitis C virus NS3/4A protease-mediated cleavage of the Toll-like receptor 3 adaptor protein TRIF. Proc Natl Acad Sci U S A 102: 2992–2997.
37. Abe T, Kaname Y, Hamamoto I, Tsuda Y, Wen X, et al. (2007) Hepatitis C virus nonstructural protein 5A modulates the toll-like receptor-MyD88-dependent signaling pathway in macrophage cell lines. J Virol 81: 8953–8966.
38. Heim MH, Moradpour D, Blum HE (1999) Expression of hepatitis C virus proteins inhibits signal transduction through the Jak-STAT pathway. J Virol 73: 8469–8475.
39. Arnaud N, Dabo S, Maillard P, Budkowska A, Kalliampakou KI, et al. (2010) Hepatitic C virus controls interferon production through PKR activation. PLoS One 5: e10575.
40. Ploss A, Evans MJ, Gaysinskaya VA, Panis M, You H, et al. (2009) Human occludin is a hepatitis C virus entry factor required for infection of mouse cells. Nature 457: 882–886.
41. Satoh T, Kato H, Kumagai Y, Yoneyama M, Sato S, et al. (2010) LGP2 is a positive regulator of RIG-I- and MDA5-mediated antiviral responses. Proc Natl Acad Sci U S A 107: 1512–1517.
42. Ishikawa H, Ma Z, Barber GN (2009) STING regulates intracellular DNA-mediated, type I interferon-dependent innate immunity. Nature 461: 788–793.
43. Dixit E, Boulant S, Zhang Y, Lee ASY, Odendall C, et al. (2010) Peroxisomes are signaling platforms for antiviral innate immunity. Cell 141: 668–681.
44. Yasukawa K, Oshiumi H, Takeda M, Ishihara N, Yanagi Y, et al. (2009) Mitofusin 2 inhibits mitochondrial antiviral signaling. Sci Signal 2: ra47.
45. Scott I (2010) The role of mitochondria in the mammalian antiviral defense system. Mitochondrion 10: 316–320.
46. Binder M, Kochs G, Bartenschlager R, Lohmann V (2007) Hepatitis C virus escape from the interferon regulatory factor 3 pathway by a passive and active evasion strategy. Hepatology 46: 1365–1374.
47. Takaoka A, Yanai H, Kondo S, Duncan G, Negishi H, et al. (2005) Integral role of IRF-5 in the gene induction programme activated by Toll-like receptors. Nature 434: 243–249.

Published November 8, 2010

JEM

Article

Identification of a polyI:C-inducible membrane protein that participates in dendritic cell–mediated natural killer cell activation

Takashi Ebihara,[1] Masahiro Azuma,[1] Hiroyuki Oshiumi,[1] Jun Kasamatsu,[1] Kazuya Iwabuchi,[2] Kenji Matsumoto,[3] Hirohisa Saito,[3] Tadatsugu Taniguchi,[4] Misako Matsumoto,[1] and Tsukasa Seya[1]

[1]Department of Microbiology and Immunology, Hokkaido University Graduate School of Medicine, Kita-ku, Sapporo 060-8638, Japan
[2]Division of Immunobiology, Institute for Genetic Medicine, Hokkaido University, Sapporo, Japan, 060-0815, Japan
[3]Department of Allergy and Immunology, National Research Institute for Child Health and Development, Setagaya-ku, Tokyo 157-8535, Japan
[4]Department of Immunology, Graduate School of Medicine and Faculty of Medicine, University of Tokyo, Bunkyo-ku, Tokyo 113-0033, Japan

In myeloid dendritic cells (mDCs), TLR3 is expressed in the endosomal membrane and interacts with the adaptor toll/interleukin 1 receptor homology domain–containing adaptor molecule 1 (TICAM-1; TRIF). TICAM-1 signals culminate in interferon (IFN) regulatory factor (IRF) 3 activation. Co-culture of mDC pretreated with the TLR3 ligand polyI:C and natural killer (NK) cells resulted in NK cell activation. This activation was triggered by cell-to-cell contact but not cytokines. Using expression profiling and gain/loss-of-function analyses of mDC genes, we tried to identify a TICAM-1–inducing membrane protein that participates in mDC-mediated NK activation. Of the nine candidates screened, one contained a tetraspanin-like sequence and satisfied the screening criteria. The protein, referred to as IRF-3–dependent NK-activating molecule (INAM), functioned in both the mDC and NK cell to facilitate NK activation. In the mDC, TICAM-1, IFN promoter stimulator 1, and IRF-3, but not IRF-7, were required for mDC-mediated NK activation. INAM was minimally expressed on NK cells, was up-regulated in response to polyI:C, and contributed to mDC–NK reciprocal activation via its cytoplasmic tail, which was crucial for the activation signal in NK cells. Adoptive transfer of INAM-expressing mDCs into mice implanted with NK-sensitive tumors caused NK-mediated tumor regression. We identify a new pathway for mDC–NK contact-mediated NK activation that is governed by a TLR signal-derived membrane molecule.

CORRESPONDENCE
Tsukasa Seya:
seya-tu@pop.med.hokudai.ac.jp

Abbreviations used: BMDC, BM-derived DC; IKK, IκB kinase; INAM, IRF-3–dependent NK-activating molecule; IPS-1, IFN promoter stimulator 1; IRF, IFN regulatory factor; mDC, myeloid DC; PRR, pattern recognition receptor; Rae-1, retinoic acid–inducible gene 1; TICAM-1, toll/IL-1 receptor homology domain–containing adaptor molecule 1; TLR, Toll-like receptor.

Natural killer (NK) cells contribute to innate immune responses by killing virus-infected or malignantly transformed cells and by producing cytokines such as IFN-γ and TNF. NK cell activation is determined by a balance of signals from inhibitory and activating receptors. Because ligands of inhibitory receptors include MHC class I and class I–like molecules, the absence of self-MHC expression leads to NK activation (Cerwenka and Lanier, 2001). Approximately 20 receptors contribute to NK activation (Cerwenka and Lanier, 2001; Vivier et al., 2008). When ligands for activating receptors are sufficiently abundant, activating signals overcome inhibitory signals.

There are two currently accepted models for in vivo NK activation. One is that NK cells usually circulate in a naive state and are activated through interaction directly with ligands for pattern recognition receptors (PRRs) expressed by NK cells or interaction with cells that express PRR ligands (Hornung et al., 2002; Sivori et al., 2004). When pathogens enter the host, innate immune sensors, such as Toll-like receptors (TLRs), RIG-I-like receptors,

T. Ebihara and M. Azuma contributed equally to this paper.
T. Ebihara's present address is Howard Hughes Medical Institute, Washington University School of Medicine, St. Louis, MO 63110.

The Rockefeller University Press $30.00
J. Exp. Med. Vol. 207 No. 12 2675-2687
www.jem.org/cgi/doi/10.1084/jem.20091573

Supplemental Material can be found at:
http://jem.rupress.org/content/suppl/2010/11/04/jem.20091573.DC1.html

Published November 8, 2010

NOD-like receptors, and lectin family proteins, which are PRRs, recognize a variety of microbial patterns (pathogen-associated molecular patterns [PAMPs]; Medzhitov and Janeway, 1997). Mouse NK cells express almost all TLRs (TLR1–3, 4, and 6–9), and some of these are directly activated by pathogens with the help of IL-12, IL-18, IFN-γ, and other cytokines (Newman and Riley, 2007). The other is that naive NK cells tend to be recruited to the draining LNs, where they are primed to be effectors with the help of mature myeloid DCs (mDC) and released into peripheral tissues (Fernandez et al., 1999). In this case, mDCs provide direct activating signals to NK cells through cell–cell contact (Gerosa et al., 2002; Akazawa et al., 2007a; Lucas et al., 2007). mDCs also produce proinflammatory cytokines and IFN-α after recognizing PAMPs (Newman and Riley, 2007). In this mDC-mediated NK activation, however, the molecules and mechanisms in mDC that are dedicated to NK activation in vivo remain to be understood.

In this study, we focused on the molecules that are induced in mDC during maturation by exposure to double-stranded (ds) RNA and the molecules involved in priming NK cells for target killing (Akazawa et al., 2007a). dsRNA of viral origin and the synthetic analogue polyI:C induce NK activation in concert with mDC in vivo and in vitro (Seya and Matsumoto, 2009). PolyI:C is recognized by the cytoplasmic proteins RIG-I/MDA5 and the membrane protein TLR3, both of which are expressed in mDC (Matsumoto and Seya, 2008). Although RIG-I and MDA5 in the cytoplasm deliver a signal to the adaptor protein IFN promoter stimulator 1 (IPS-1; also known as MAVS, VISA, and Cardif) on the outer membrane of the mitochondria (Kawai et al., 2005; Meylan et al., 2005; Seth et al., 2005; Xu et al., 2005), TLR3 in the endosomal membrane recruits the adaptor protein toll/IL-1 receptor homology domain–containing adaptor molecule 1 (TICAM-1)/TRIF (Oshiumi et al., 2003a; Yamamoto et al., 2003a). Both adaptor proteins activate TBK1 and/or IκB kinase (IKK) ε, which phosphorylate IFN regulatory factor (IRF) 3 and IRF-7 to induce type I IFN (Sasai et al., 2006). We previously showed that the TLR3–TICAM-1 pathway in mDC participates in inducing anti-tumor NK cytotoxicity by polyI:C (Akazawa et al., 2007a). mDC matured with polyI:C can enhance NK cytotoxicity through mDC-NK cell–cell contact (Akazawa et al., 2007a). Therefore, we hypothesized that an unidentified protein is up-regulated on the cell surface of mDC through activation of the TLR3–TICAM-1 pathway, and this protein enables mDC to interact with and activate NK cells. This is the first study identifying an IRF-3–dependent NK-activating molecule, which we abbreviated INAM. INAM is a TICAM-1–inducible molecule on the cell surface of BM-derived DCs (BMDCs) that activates NK cells via cell–cell contact. Our data imply that mDCs harbor a pathway for driving NK activation that acts in conjunction with dsRNA and TLR3.

RESULTS

TICAM-1/IRF-3 signal in BMDCs augments NK activation

An in vitro system for evaluating NK activation through BMDC-NK contact was established for this study (Fig. 1 A). A mouse melanoma cell subline B16D8, which was established in our laboratory as a low H-2 expressor (Mukai et al., 1999), was used as an NK target. PolyI:C, WT BMDC, and NK cells were all found to be essential for NK-mediated B16D8 cytolysis in the in vitro assay (Fig. 1 A). PolyI:C-mediated NK activation was at baseline levels in a transwell with a 0.4-μm pore, suggesting the importance of direct BMDC-NK contact for this cytolysis induction (Fig. 1 A). When WT BMDCs were replaced with TICAM-1$^{-/-}$ BMDCs in this system, polyI:C-mediated NK activation was partly abolished (Fig. 1 B; and Fig. S1, A and B). TICAM-1 of BMDC was involved in driving NK activation, and ultimately B16D8 cells were damaged by BMDC-derived NK cells (Fig. 1 B). PolyI:C-mediated NK activation occurred even when WT NK cells were replaced with TICAM-1$^{-/-}$ NK cells (Fig. 1 B), which means that NK activation barely depends on the TICAM-1 pathway in NK cells.

PolyI:C-activated splenic NK cells were i.p. injected into B6 mice to kill B16D8 cells ex vivo, which is consistent with previous studies (McCartney et al., 2009; Miyake et al., 2009), and this polyI:C-mediated NK activation was markedly reduced in IPS-1$^{-/-}$ mice established in our laboratory (Fig. S1 C), suggesting that NK cell activation is induced via not only the TICAM-1 pathway but also the IPS-1 pathway, which was largely comparable with previous studies (McCartney et al., 2009; Miyake et al., 2009). IPS-1 in BMDC was more involved in polyI:C-driven NK cytotoxicity than TICAM-1 but almost equally contributed to NK-dependent IFN-γ induction to TICAM-1 in our setting (Fig. S1 B). In addition, the serum level of IL-12p40 in polyI:C-treated mice was largely dependent on TICAM-1 (Fig. S1 D; Kato et al., 2006; Akazawa et al., 2007a). In the supernatant of polyI:C-stimulated BMDC and the serum samples from polyI:C-treated mice, IL-12p70 was not detected by ELISA (unpublished data). These results suggest that polyI:C activates NK cells largely secondary to mDC maturation, which is sustained by the IPS-1 or TICAM-1 pathway of mDC. Even though NK cells express TLR3, they are only minimally activated by polyI:C alone. Signaling by TICAM-1 in BMDC can augment NK cytotoxicity and IFN-γ production via BMDC/NK contact.

The TICAM-1 pathway activates the transcription factor IRF-3. More precisely, exogenous addition of polyI:C can activate endosomal TLR3 and cytoplasmic RIG-I/MDA5. RIG-I/MDA5 assembles the adaptor IPS-1, which in turn recruits the NAP1–IKK-ε–TBK1 kinase complex and activates both IRF-3 and IRF-7 (Fitzgerald et al., 2003; Yoneyama et al., 2004). For this reason, we examined the role of IRF-3 and IRF-7 in BMDC for activation of NK cells by polyI:C. Activation of IRF-3, but not IRF-7, was required for BMDC to induce NK cytotoxicity (Fig. 1 C). IL-2 (Zanoni et al., 2005), IFN-α (Gerosa et al., 2002), and trans-presenting IL-15 (Lucas et al., 2007) induced by BMDC are reported to be key cytokines for BMDC-mediated NK activation in response to polyI:C. However, even with normal levels of IFN-α production and IL-15 expression (Fig. 1, D and E), TICAM-1$^{-/-}$ BMDCs failed to induce full NK cytotoxicity (Fig. 1 B). In contrast, IRF-7$^{-/-}$ BMDCs, which have impaired IFN-α and IL-15

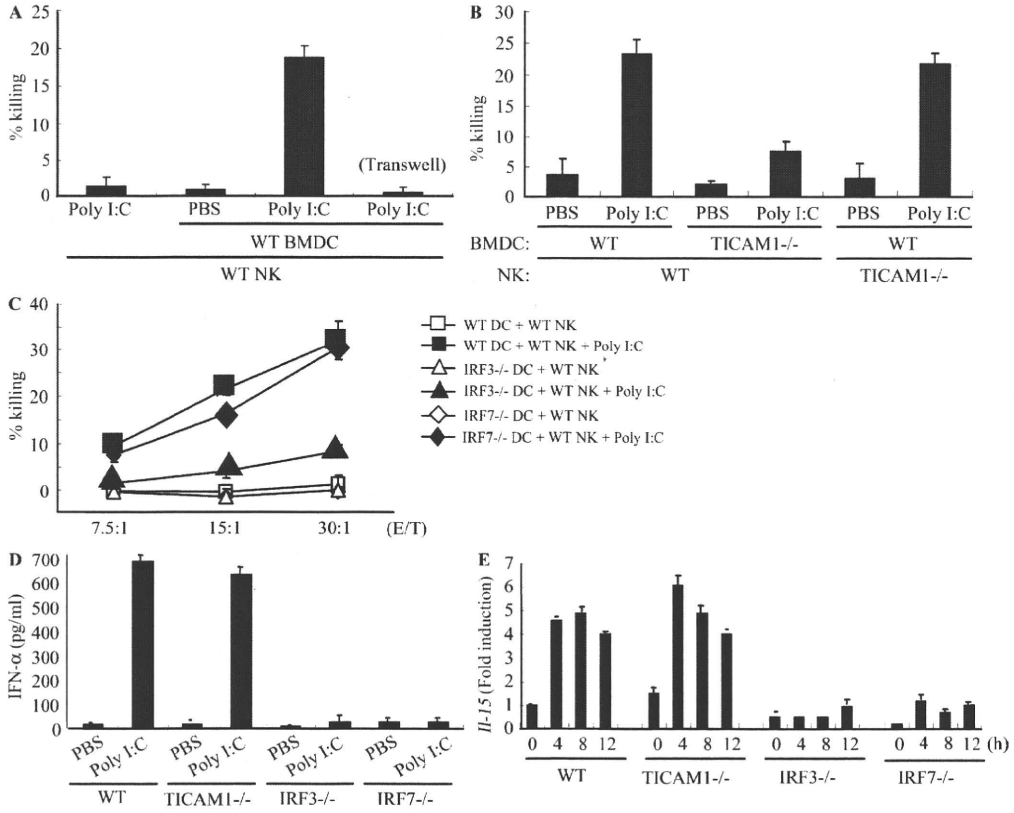

Figure 1. IRF-3 in BMDC controls the capacity to activate NK cells in response to polyI:C. (A and B) WT or TICAM-1$^{-/-}$ NK cells were co-cultured with WT or TICAM-1$^{-/-}$ BMDC in the presence of 10 µg/ml polyI:C for 24 h. NK cytotoxicity against B16D8 was determined by standard ^{51}Cr release assay. E/T = 30. (C) WT NK cells were co-cultured with WT (□, ■), IRF-3$^{-/-}$ (△, ▲), or IRF-7$^{-/-}$ (◇, ◆) BMDC in the presence (■, ▲, ◆) or absence (□, △, ◇) of 10 µg/ml polyI:C for 24 h. NK cytotoxicity against B16D8 was determined by standard ^{51}Cr release assay at the indicated E/T ratio. (D) ELISA of IFN-α in cultures of WT, TICAM-1$^{-/-}$, IRF-3$^{-/-}$, and IRF-7$^{-/-}$ BMDC treated with 10 µg/ml polyI:C for 24 h. (E) Quantitative RT-PCR for IL-15 expression in BMDC stimulated with 10 µg/ml polyI:C. All data are means ± SD of duplicate or triplicate samples from one experiment that is representative of three.

expression, fully activated NK cells (Fig. 1, C–E). Hence, in BDMCs, the TICAM-1–IRF-3 pathway, rather than other cytokines, appears to induce cell surface molecules that mediate BMDC/NK contact and evoke NK cytotoxicity.

Identification of INAM

To identify the NK-activating cell surface molecule on BMDC, we performed microarray analysis on polyI:C-stimulated BMDC prepared from TICAM-1$^{-/-}$ and WT mice. The results yielded nine TICAM-1–inducible molecules with transmembrane motifs (Table S1). Six were induced in an IRF-3–dependent manner, whereas three were still induced in IRF-3$^{-/-}$ BMDC. The NK-activating ability of the products of these genes was investigated by introduction of lentivirus expression vector into IRF-3$^{-/-}$ BMDC. BMDCs with the transduced genes were co-cultured with WT NK cells and polyI:C, and the NK-activating ability was evaluated by determining IFN-γ in the 24-h co-culture. NK cells, but not the gene-transduced BMDCs, produced IFN-γ in the presence of polyI:C. Finally, we identified a tetraspanin-like molecule that satisfied our evaluation criteria (IFN-γ and cytotoxicity) on the mDC-NK activation and named this molecule INAM. INAM clearly differed from other tetraspanins like CD9, CD63, CD81, CD82, and CD151 in the predicted structure. Mouse INAM is a 40–55-kD protein with one N-glycosylation site and possesses four transmembrane motifs (Fig. 2, A and B). Western blotting analysis of INAM-transfected cells under nonreducing conditions showed no evidence of multimers (Fig. 2 B). The N-terminal and C-terminal regions of INAM are in the cytoplasm because anti-Flag antibody did not detect C-terminal Flag-tagged INAM until cells were permeabilized (unpublished data).

Alignment of the predicted amino acid sequence of mouse INAM with that of the human orthologue revealed that the two INAMs shared a 71.7% amino acid identity. INAM is also called FAM26F (Table S1) and is in the FAM26 gene family (Bertram et al., 2008; Dreses-Werringloer et al., 2008). Sequence database searches identified six mouse INAM paralogs. Although FAM26A/CALHM3, FAM26B/CALHM2, and FAM26C/CALHM1 are located on chromosome 19, FAM26D, FAM26E, and FAM26F/INAM are on chromosome 10. Only INAM was inducible with TLR agonists (unpublished data). All FAM26 family proteins have three or four transmembrane motifs predicted by the TMHMM Server (version 2.0). Human CALHM1 has a conserved region (Q/R/N site)

Published November 8, 2010

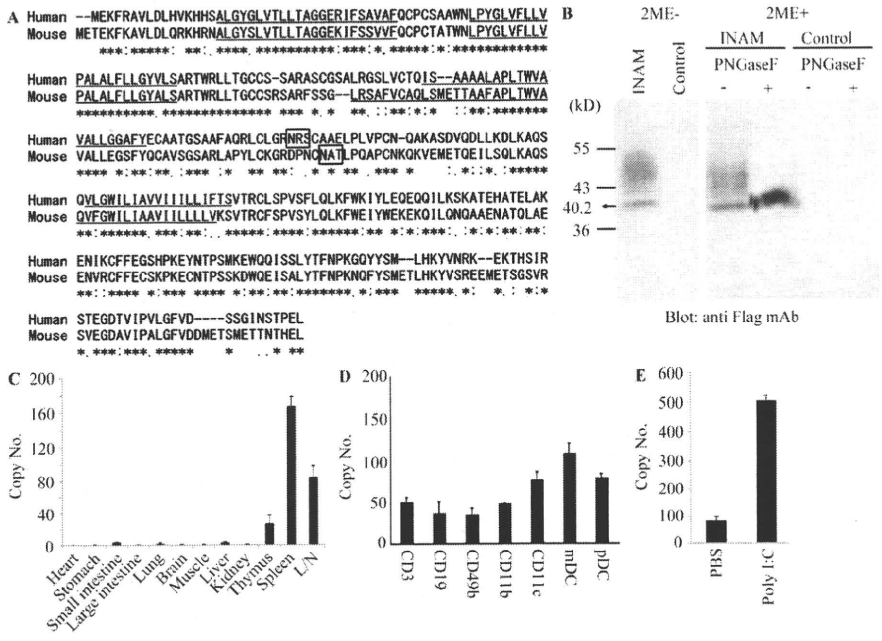

Figure 2. Sequence alignment of INAM and expression of INAM. (A) Sequence alignment of human and mouse INAM. Asterisks, identical residues; double dots, conserved substitutions; single dots, semiconserved substitutions; box, N-glycosylation site; underline, transmembrane motif. (B) Immunoblot analysis of lysates of 293FT cells transfected with plasmid encoding Flag-tagged INAM. PNGase, *N*-glycosidase. 2ME, 2-mercaptoethanol. (C and D) Quantitative RT-PCR for INAM expression in mouse tissue (C) and spleen cells (D). $CD3^+$, $CD19^+$, $DX5^+$, $CD11b^+$, $CD11c^+$, mDC ($CD11c^+PDCA1^+$), and plasmacytoid DC (pDC; $CD11c^+PDCA1^+$) cells were isolated from splenocytes by cell sorting. Data are expressed as copy number per 10^4 copies of HPRT. Data shown are means ± SD of triplicate samples from one experiment that is representative of three. (E) Augmented INAM expression in LN cells after polyI:C stimulation. WT mice were i.p. injected with 100 µg polyI:C or control buffer. After 24 h, inguinal, axillary, and mesenteric LN were harvested and RNA was extracted from the LN cells. The levels of the INAM mRNA were measured by real-time PCR. The results were confirmed in two additional experiments. Data represent mean ± SD.

with ion channel properties at the C-terminal end of the second transmembrane motif that controls cytoplasmic Ca^{2+} levels (Dreses-Werringloer et al., 2008). However, the Q/R/N site was not found in INAM. CALHM1, 2, and 3 are highly expressed in brain. Quantitative RT-PCR revealed that INAM expression was high in spleen and LNs but low in thymus, liver, lung, and small intestine (Fig. 2 C), although expression of the other two FAM26 family members from chromosome 10 was highest in brain (not depicted). All splenocytes examined ($CD3^+$, $CD19^+$, $DX5^+$, $CD11b^+$, $CD11c^+$, mDCs [$CD11c^+$ $PDCA1^-$], and plasmacytoid DCs [$CD11c^-PDCA1^+$]) expressed INAM to some levels (Fig. 2 D). The INAM expression was inducible by polyI:C in LN cells (Fig. 2 E); the induction levels were more prominent in myeloid cells than in lymphocytes in the LNs (Fig. S2 A). $NKp46^+$ and $DX5^+$ NK cells also expressed INAM with low levels and the levels were mildly increased by polyI:C stimulation (Fig. S2 A and not depicted). Notably, only $CD45^+$ cells expressed INAM, which excludes the participation of contaminating stromal cells in the INAM up-regulation (Fig. S2 B).

BMDC INAM activates NK cells

WT and IRF-$7^{-/-}$ BMDCs induced high NK cytotoxicity in response to polyI:C, whereas TICAM-$1^{-/-}$, IPS-$1^{-/-}$, and IRF-$3^{-/-}$ BMDC showed less NK activation (Fig. 1, B and C; and Fig. S1). INAM expression profile by polyI:C stimulation was then examined using WT, IRF-$3^{-/-}$, IRF-$7^{-/-}$, and TICAM-$1^{-/-}$ BMDCs. Stimulation with polyI:C induced INAM at normal levels in IRF-$7^{-/-}$ BMDC but at decreased levels in IRF-$3^{-/-}$ and TICAM-$1^{-/-}$ BMDC (Fig. 3 A). The expression profiles of INAM in polyI:C-stimulated BMDC were in parallel with those inducing NK activation. BMDCs express a variety of TLRs (Iwasaki and Medzhitov, 2004), but other TLR ligands, Pam_3CSK_4 for TLR1/2, Malp2 for TLR2/6, and CpG for TLR9, barely induced INAM on BMDC. High induction of INAM was observed in BMDC stimulated with LPS as well as polyI:C (Fig. 3 B), both of which can activate TICAM-1 to induce IRF-3 and IFN-α activation (Fitzgerald et al., 2003; Oshiumi et al., 2003a,b; Yamamoto et al., 2003a,b). Because INAM is an IFN-inducible gene (Fig. 3 B), INAM induction may be amplified by type I IFNs.

We next examined whether INAM was localized to the cell surface membrane in BMDC. Immunofluorescence analysis showed Flag-tagged INAM on the cell surface of BMDC. Plasma membrane expression of INAM was also confirmed by cell surface biotinylation (Fig. S3). Although the lentivirus inefficiently infected BMDC, GFP expression levels were similar in cells with control virus and those with INAM-expressing virus (Fig. 3 C). Transduction efficiency and expression from the lentivirus vector were adjusted using GFP expression (not depicted), and surface INAM expression was further confirmed with BMDC, NK cells, and INAM-expressing BaF3 (INAM/BaF3) cells, in some cases using polyclonal antibody (Ab) against INAM (Fig. S4).

We then examined whether overexpressing INAM resulted in signaling that directed BMDC maturation and production of cytokines, including IFN-α and IL-12p40, which are reported to enhance NK activity (Gerosa et al., 2002; Sivori et al., 2004; Lucas et al., 2007). The status of INAM-transduced BMDC was assessed by CD86 expression and cytokine production, and no significant differences in these maturation markers were seen in BMDC overexpressing INAM (Fig. S5). In the same setting, no IL-12p70 was